ARVIN/CALSPAN

UPDATING THE SMITH-FEDDES MODEL

Calspan Report No. 7330-1

C. William Rogers
James T. Hanley
Eugene J. Mack

FINAL REPORT

Contract No. N00228-84-C-3157

June 1985

Prepared for:

Dr. Paul M. Tag
Naval Environmental Prediction Research Facility
Monterey, CA 93943

CALSPAN CORPORATION P O BOX 400 BUFFALO, NEW YORK 14225

UNCLASSIFIED

SECURITY CLASSIFICATION OF THIS PAGE (When Data Entered)

REPORT DOCUMENTATION PAGE		READ INSTRUCTIONS BEFORE COMPLETING FORM
1. REPORT NUMBER	2. GOVT ACCESSION NO.	3. RECIPIENT'S CATALOG NUMBER
4. TITLE (and Subtitle) Updating the Smith-Feddes Model		5. TYPE OF REPORT & PERIOD COVERED Final Report September 1984-June 1985
		6. PERFORMING ORG. REPORT NUMBER 7330-1
7. AUTHOR(s) C.W. Rogers, J.T. Hanley and E.J. Mack		8. CONTRACT OR GRANT NUMBER(s) N00228-84-C-3157
9. PERFORMING ORGANIZATION NAME AND ADDRESS Arvin/Caslapn Advanced Technology Center P.O. Box 400 Buffalo, NY 14225		10. PROGRAM ELEMENT, PROJECT, TASK AREA & WORK UNIT NUMBERS
11. CONTROLLING OFFICE NAME AND ADDRESS Regional Contracting Department Naval Supply Center Oakland, CA 94625		12. REPORT DATE June 1985 13. NUMBER OF PAGES 85
14. MONITORING AGENCY NAME & ADDRESS(if different from Controlling Office) Naval Environmental Prediction Research Facility Monterey, CA 93943		15. SECURITY CLASS. (of this report) UNCLASSIFIED 15a. DECLASSIFICATION/DOWNGRADING SCHEDULE

16. DISTRIBUTION STATEMENT (of this Report)

Approved for public release; distribution is unlimited.

17. DISTRIBUTION STATEMENT (of the abstract entered in Block 20, if different from Report)

18. SUPPLEMENTARY NOTES

19. KEY WORDS (Continue on reverse side if necessary and identify by block number)

Cloud Microphysics Measurements	Moist Adiabatic Process
Computer Model	RTNEPH
Cloud Liquid Water	Smith-Feddes Model
Cloud Ice	Bibliography of Cloud Microphysics Measurements
Cloud Drop-Size Distribution	Entrainment

20. ABSTRACT (Continue on reverse side if necessary and identify by block number)

The Smith-Feddes (S-F) model, which provided cloud and precipitation water content and drop-size distribution from 3DNEPH cloud input, was modified to accept cloud information in the RTNEPH format produced at the Air Force Global Weather Center and to incorporate more rigorous specification of microphysics. The computer code for this modified model was installed for operational use at the Navy's Fleet Numerical Oceanography Center (FNOC).

DD FORM 1 JAN 73 1473

UNCLASSIFIED

SECURITY CLASSIFICATION OF THIS PAGE (When Data Entered)

20. Continued

The cloud microphysics of the model, which included a table of cloud maximum condensed moisture by temperature, specification of the relative amount of supercooled water and ice in cloud, and designation of drop-size distributions in cloud, were examined for overall adequacy, accuracy and representativeness with respect to observations acquired since development (~1973) of the model. Primarily because the S-F condensed moisture table specified same water content value for cumulus clouds without regard to cloud depth, we modified the model so that it computes condensed moisture content via moist adiabatic ascent for all noncirriform clouds. For cumuliform clouds the adiabatic water content is reduced to account for entrainment of environmental air.

The drop size distributions for liquid type clouds were found to be incorrectly specified; corrected values were derived, and these were also installed in the computer code.

In the original S-F model, the cloud water between the liquid and ice phases in an individual cloud had been incorrectly developed from frequency of occurrence of water and water-and-ice in clouds. However, the probability (i.e., frequency of occurrence) that the cloud was all water can be specified, and the S-F model now provides that information as output.

TABLE OF CONTENTS

LIST OF TABLES

LIST OF FIGURES

Section 1
INTRODUCTION AND SUMMARY

1.1 INTRODUCTION

Under Contract No. N00228-84-C-3157 with the Naval Environmental Prediction Research Facility, Calspan Corp. performed an update of the Smith-Feddes (S-F) computer model which converts cloud observations into vertical profiles of cloud water and drop size distribution. This update involved two main phases. The first phase dealt with modification of the model to accept as input an improved cloud depiction, the so-called RTNEPH, as produced by the Air Force Global Weather Center. The modified model was temporarily installed at Fleet Numerical Oceanography Center (FNOC), Monterey, CA.

The second phase involved examination of the cloud microphysics parameterizations incorporated in the model, i.e., cloud moisture content vs. temperature by cloud type, cloud particle-size distributions and relative amounts of liquid and ice in cloud. Where the parameterizations were inaccurate or where recent observations indicated changes should be made, the model was modified. This final, updated model was then installed on the FNOC computer system to replace the temporary version. In addition, a User's Guide was prepared for the modified model according to DOD Standard 7935.1s, 13 September 1977 (superseded by DOD Std-7935, 15 February 1983).

It must be pointed out that the documentation for the microphysics portion of the original S-F model is woefully inadequate. Although many references are provided, explicitly which data were used, and how they were used, to derive the parameterizations are indeterminable. Evaluation of the microphysics parameterization was made extremely difficult by incomplete documentation. To examine the microphysics it was often necessary to assume, from the context of the documentation discussion, both the observed data used and the path of analysis, from these data to the parameterized microphysics. For aid in any future development of this model, we have clearly indicated our analysis approaches and the data which entered these analyses.

Much of the microphysics research effort dealt with assessing whether observations of cloud microphysics, which were obtained since the S-F model was developed (- 1973), supported or required changes in the S-F microphysics parameterizations. An extensive literature survey was carried out using computerized data bases, NTIS for government reports and INSPEC for refereed papers. In addition, current literature was monitored during the course of the contract for any appropriate publications. Thus, the set of microphysics observations we worked with represents as complete and up-to-date a set as we could amass.

1.2 MODIFICATION OF S-F MODEL TO ACCEPT RTNEPH CLOUD DATA FORMAT

The Smith-Feddes computer model as supplied to Calspan from the Naval Surface Weapons Center (NSWC) had to be modified to run on the Calspan computer facility. This FORTRAN computer code had been prepared for NSWC from the original COBOL-FORTRAN code to run from their specifically tailored input data base of temperature, terrain and 3DNEPH cloud format (Dykton et. al, 1984; Brown, 1983). Since output from the RTNEPH version had to be compared to output from the 3DNEPH version to insure continuity, we had to redesign the code to accept inputs as available to us. This meant development of unpacking routines for both the 3DNEPH and terrain data tapes, as well as code to specify the geometric heights of the vertical cloud layers relative to the underlying terrain. Obviously, an unpacking routine for the RTNEPH data tape was also developed. Finally, a temperature input routine using temperature observations at standard pressure levels was constructed.

The original Smith-Feddes model entered cloud type and cloud cover percentage into predetermined and prespecified fixed geometric height intervals, i.e. vertical layers which were defined by geometric heights above mean sea level and which accounted for the underlying terrain height (3DNEPH format). The RTNEPH cloud data format provides only the height of the base and top of a cloud deck. Consequently, the RTNEPH version of the S-F model simply redefined the top height of the geometric layer into which the RTNEPH cloud deck protruded and the bottom height of the geometric layer into which it extended. Any geometric layers in between remain unchanged, and only the encompassing layers are redefined to match the reported bottom and top height of the cloud deck. In addition, the program converts the RTNEPH cloud-type numerical code to the S-F cloud-type numerical code.

The S-F microphysics code is tightly structured about the geometric layer concept, with the controlling DO LOOPS and IF statements keyed to numbered geometric layers. Maintaining this structure, and inserting the RTNEPH *cloud deck height* information into it, greatly simplified adapting the S-F code to handle the RTNEPH format.

1.2.1 Installation of RTNEPH Version of S-F at FNOC

Installation of the modified code on the FNOC computer involved two efforts, the first of which was the development of unpacking routines to extract the data from the RTNEPH and terrain tapes. These routines utilize the FNOC library routines, BRPK and BXMT, to manipulate the byte strings contained in the tape data records and to extract the cloud and terrain data for the desired geographic location.

The second effort concerned obtaining the temperature vs. height for input to the program. An FNOC library program, PNTDAT, provides the temperatures for a data point defined by latitude and longitude coordinates. The data base accessed by this routine is the most recent FNOC standard, 12-hour upper air analyses. PNTDAT is a stand alone program and is independently run prior to running the S-F program.

1.3 MICROPHYSICS PARAMETERIZATIONS

For each geometric layer containing cloud, the original S-F model provided as output the following layer-mean parameters:

1. total condensed moisture content
2. *respective amounts of cloud liquid and ice*
3. when the cloud is precipitating, the respective amounts of liquid and ice precipitation in the cloud as well as in precipitation from the base of the lowest cloud deck to the earth's surface
4. for the categories in 2.) and 3.), a water droplet and/or ice particle number concentration distribution.

Under the second phase of the contract we examined the parameterizations, used in providing the microphysical output from the cloud data input, for accuracy and empirical up-to-dateness and made modifications where required. The results of this examination are summarized below.

1.3.1 Total Condensed Moisture Content

In the original S-F model, total condensed moisture content (CMC) is provided from a table in which CMC is empirically specified as a function of cloud type and temperature. Ten cloud types and ten temperature intervals produce a 100 entry table. Based on the more recent measurements, 22 values were changed, 22 values were supported, and 56 values could be neither supported nor changed.

For convective type clouds, the empirical CMC vs. temperature approach assigns the same CMC for a given temperature no matter at what height in the cloud the temperature occurs. Since the water content of convective cloud is related to liquid water content generated during adiabatic ascent, the empirical approach seemed inadequate to specify the CMC of convective clouds. Consequently, in consultation with the COTR, we agreed to implement an adiabatic approach for convective clouds. Because of entrainment through the sides of the cloud, the CMC is specified as a fraction of the adiabatic value.

While the adiabatic approach was initiated to provide a more sound physical basis for deeper convective cloud types, it was extended to all non-ice type clouds, including both stratiform and the other cumuliform clouds, stratocumulus and altocumulus. For the cumuliform cloud types, adiabatic CMC values are subjected to the same reduction for entrainment as are Cu and Cb. For stratus clouds, the unreduced adiabatic value is used.

1.3.2 Percentages of Liquid and Ice in a Given Cloud

Our analysis indicated that the algorithms used to provide percentages of liquid and ice in cloud were based on an incorrect interpretation of data.

The data quoted by Smith (1974) came from Khrgian (1963). Close examination of these data showed that they were the percentage of <u>all</u> clouds at a

given temperature which contained liquid water only, not the percentage of cloud condensed moisture which was liquid at a given temperature. No data could be found which provide the relative percentages of liquid and ice within a specific cloud containing both phases. In discussion with the COTR it was agreed that the percentage computed in the S-F program would henceforth be reported in the output, but labeled as the probability that the cloud contained liquid water only. The same approach is used for precipitation in cloud.

1.3.3 Drop Size Distributions

The drop size distributions are produced via a parameterized equation which requires for each cloud type: 1) the fraction of CMC which occurs at the mode in the distribution, 2) the droplet size of the mode, and 3) the volume of the droplet at the mode size. Our analysis concluded that these parameterizations were appropriate for cirriform clouds and incorrect for all liquid type clouds.

Comparison between the parameterized magnitude of the droplet size at which the peak occurs and observations of this peak indicated that many of the parameterized values were too small. To compute an independent set of values of the peak location, we followed the procedure outlined by Feddes (1974) which was to compute liquid water content in a drop size interval and then divide by the drop mass to obtain the number of drops. The input data to these computations were relative drop-size distributions (Diem, 1948) referenced by Smith (1974). The resulting parameterizations were compared against observed peak locations and total droplet concentrations for the various cloud types (from recent literature) and were judged to be representative. The revised parameterizations were entered into the S-F computer code.

The derivation of the precipitation drop distribution from Kessler (1969) was verified to be correct.

1.3.4 Cloud Cover Percentage

The RTNEPH input cloud observations (base, top, cloud type, and cloud cover percentage) represent conditions within a 25 x 25 n. mi. square column of the earth's atmosphere. A continuing question has been the interpretation and use of the

cloud cover percentage in the S-F model. In the original model supplied by NSWC, the CMC obtained from the S-F microphysics parameterizations was multiplied by the cloud cover percentage and the reduced value labeled as CMC. This approach produced area averaged CMC and drop size distribution. Such area averages might be appropriate for studies of world wide climatological cloud cover or long term radiation budget studies. However, it was not our understanding that this approach was necessarily best suited to NSWC's intended use of the S-F model.

In consultation with the COTR it was decided that the full CMC value (appropriately obtained from either the adiabatic or the tabular approach) would be printed in the output. The cloud cover percentage would also be printed out and labeled as the probability of encountering the CMC and its drop size distribution. With this format, NSWC now has both an estimate of the microphysical conditions that would be realized in the cloudy portions within the 25 x 25 n. mi. square, as well as the probability of encountering those conditions within the square. If area average values are desired, they can readily be determined from the above output data.

1.4 SUMMARY OF MODIFICATIONS TO THE S-F MODEL

NSWC had an operational computer model, the so-called Smith-Feddes (S-F) Model which provided vertical profiles of cloud moisture content and drop-size distribution from 3DNEPH world wide cloud observations. Calspan Corporation engaged in a two phase research effort to provide an updated operational model to run on the FNOC computer installation. Phase 1 involved modifying the existing computer model to accept cloud input observations form a new format (RTNEPH). Phase 2 was to modify, if necessary in light of recent measurements, the cloud physical and thermodynamical parameterizations inherent in the model.

Phase 1 was rather straightforward and involved additions to the computer code to preprocess the RTNEPH cloud base and top height data into a format which could be input to the existing S-F microphysics computer code, and to unpack the terrain height and RTNEPH input tapes.

Phase 2 involved a literature search for reports and papers published during the last 10 years which concentrated primarily on observations of cloud microphysical and thermodynamical properties. Central to the original S-F model was a table which

specified, by cloud type, condensed moisture content (CMC) as a function of temperature within the cloud layer. Because of the key role played by this table in the S-F approach, substantial early effort was expended in verification and modification of the table's entries, based on the new observations. When the parameterization of vertical profiles of CMC was examined it became clear that for Cu and Cb the combined effect of invariant CMC values (with cloud layer temperature) and CMC profiles derived from fractional heights within the cloud deck led to identical CMC values and profiles within both shallow and deep cumulus clouds. This situation contradicted both observation and theoretical computations of condensation produced during moist adiabatic ascent.

To better describe CMC in Cu and Cb clouds, we developed and installed S-F computer code which calculates the CMC produced by condensation which occurs during moist adiabatic ascent, and reduced this CMC to account for entrainment as a function of height above cloud base. This entire procedure is also applied to Sc and Ac clouds. For stratiform cloud (St, Ns and As), the adiabatically generated CMC is used at its full value since entrainment is relatively unimportant in these wide spread layered clouds. For cirriform (ice) clouds, the model still obtains CMC values via the S-F table. We feel the approach described above provides the best overall specification of CMC for the S-F model given NSWC's current application and the level of sophistication of the cloud input data, i.e. average conditions over a 25 x 25 n mi square on the earth's surface.

With regard to the data being averages over a 25 x 25 n mi square area, we, with the approval of the COTR, respecified the use of the cloud cover percentage by the S-F model. As the model provides CMC and drop size distribution for layer(s) within a column of unit area, the cloud cover percentage now is interpreted as the probability of encountering these cloud conditions within the 25 x 25 n mi square area.

The original specification of S-F relative amounts of water and ice in noncirriform cloud (at temperatures between 0° and -40°C) was based on an incorrect interpretation of data, and no data set could be found in current or past literature from which to compute these percentages. However the original S-F data can be used to specify the probability that a given cloud is all liquid water, and this probability is now provided in the S-F output.

The drop size distributions for the water type clouds were found to be incorrectly parameterized in S-F. Correct parameterizations were derived primarily from Diem's (1948) data and provided mode radii and total number concentration (for observed CMC values) which matched many observations. Situations in which the parameterized values did not match observations appear to be related to the variation of cloud nuclei populations among different geographic locations. The data used to derive the drop distribtions were taken from observations obtained in continental Europe. Because of the variation in cloud nuclei populations, particularly in the boundary layer, these European parameterizations are not completely representative of other geographical areas, such as oceanic regions.

Our primary recommendation for further improvement of the microphysics specification of the S-F model would be to parameterize at least low level rooted clouds (St, Sc and Cu) on a geographical basis to account for regional variations in cloud nuclei populations. The computer code would be changed to label the latitude-longitude input in terms of a geographic or earth's surface-type identifier so that the input location could be matched with its appropriate drop size distribution. Such an improvement would be compatible with the current overall sophistication level of the S-F model microphysics and the cloud data input produced by the RTNEPH format.

Section 2

MODIFICATION OF SMITH-FEDDES COMPUTER MODEL TO ACCEPT NEW FORMAT FOR INPUT DATA

2.1 INTRODUCTION

Under this contract Calspan Corporation conducted a multi-task research program designed to provide at FNOC an operational model which provides vertical profiles of cloud and precipitation liquid water content and drop size distributions based on cloud-cover input data. The starting point for this work was an existing computer program which used the Smith-Feddes cloud microphysics parameterizations (Smith, 1974; Feddes, 1974) for simulating condensed atmospheric moisture. The original Smith-Feddes model obtained its cloud input from the global three-dimensional cloud fields produced by the 3DNEPH computer program run at AFGWC. In early 1985, AFGWC discontinued the 3DNEPH program in favor of the RTNEPH program, which provides cloud data in a different format than in the 3DNEPH program. Since operational computer models run at FNOC must satisfy a memory size criteria, the Task 1 effort was to insure that the final computer program met this requirement. Task 2 was to modify the Smith-Feddes computer code to handle the RTNEPH format.

2.2 ADHERENCE TO CENTRAL MEMORY LIMIT AT FNOC

The central memory limit for operational programs run at FNOC is 110000 octal (36864 decimal). The Smith-Feddes, 3DNEPH computer code delivered to Calspan already met this size requirement (i.e. 21727 decimal); however, this code did not contain routines for unpacking the cloud-data magnetic tape or for operationally obtaining vertical temperature profiles, the inclusion of which might increase the operational RTNEPH program's size beyond the 110000 octal ceiling. Thus, as planned, Task 1 efforts were directed at reducing the size of the basic 3DNEPH S-F computer program to insure that the final operational RTNEPH program would meet FNOC memory-size criteria.

The original model was designed to input cloud and geometric height data for a 64 by 64 grid box (4096 grid points), thus requiring many large three- dimensional arrays. Each program execution allowed for calculation of vertical profiles of condensed

moisture parameters for only 25 of the 4096 grid points, thus never using large portions of the data in the three-dimensional arrays. An obvious way to reduce the size of the code was to process only one grid point at a time and thereby to convert the three-dimensional arrays to one-dimensional arrays. This approach was further supported by the fact that, the format of the RTNEPH computer data tapes indicated that, to minimize the central memory needed to unpack the cloud-data tape, only one grid point at a time should be processed. Therefore, in order to insure that the operational RTNEPH program with its unpacking programs would not exceed FNOC's maximum ceiling, we designed the RTNEPH operational computer code to process one grid point at a time.

A requirement of Task 1 was to compare results of the pared-down model with those from the original model. This requirement, initially relieved by the 3DNEPH model being small enough, was reinstated by our decision to go to a single grid point model. The comparison of results was one of a series of checks (Task 2 and Task 3 contain similar comparisons) designed to insure that each evolutionary modification from 3DNEPH model to RTNEPH model provided continuity in results between current and original model versions. The sequence of modification steps we chose was to first modify the three-dimensional array, 3DNEPH version to a three-dimensional array, RTNEPH version, and second to produce the one-dimensional array, single grid point RTNEPH version. This sequence of modifications allowed for the isolation of errors which may arise from program modifications involved in conversion from 3DNEPH to RTNEPH cloud input format.

As a result of the Task 1 effort, the version of an RTNEPH model, produced under Task 2 efforts, satisfied the memory size criterion for operational models on FNOC's computer. The final model which contains the revised microphysics also satisfies this size criterion.

2.3 MODIFICATION OF SMITH-FEDDES COMPUTER MODEL TO ACCEPT RTNEPH CLOUD DATA

The Smith-Feddes computer model consists of two major sections, the microphysics code and the input/output code. The microphysics code produces vertical profiles of liquid water content and drop size distribution based on cloud type, cloud height, ground elevation and vertical temperature structure provided by the input code.

In the original Smith-Feddes model, the microphysics code was tailored to operate on the 3DNEPH cloud format. In modifying the Smith-Feddes model to accept the RTNEPH cloud data format, we decided to design a preprocessor section which would reformat the RTNEPH cloud height information to look like the 3DNEPH cloud height structure, with no loss of the flexibility inherent in the RTNEPH cloud depiction.

Basically the preprocessor converts the contiguous, fixed heights of the 3DNEPH geometric layers (the bottom six are relative to ground evelation while the top nine are relative to mean sea level, the 15 layers covering the atmosphere from ground level to lower stratosphere) to the variable heights provided by the RTNEPH cloud data. As an illustration, consider the following example in Table 1:

Table 1

Comparison of 3DNEPH geometric cloud layer heights converted to RTNEPH geometric cloud layer heights.

INPUT DATA RTNEPH Cloud Heights(m)		3DNEPH Fixed Layer Heights(m)				RTNEPH Cloud Layer Heights(m)			
Bottom	Top	Layer	Bottom	Mid	Top	Layer	Bottom	Mid	Top
800	1600	7	1000	1250	1500	7	800	1200	1600
Clear	Clear	8	1501	2000	2500	8	1601	2100	2599
2600	3900	9	2501	3250	4000	9	2600	3250	3900

As can be seen by the example, the effect of this preprocessing is to redefine the geometric heights of the bottom and top of the numbered layers, for the specific cloud decks present in the RTNEPH cloud data.

In the RTNEPH S-F model, Subroutine (S/R) RTNPH reads and unpacks the RTNEPH cloud data tape, decodes the cloud base and top heights (through S/R CLDTB, which also computes the maximum cloud top and minimum cloud base) and converts RTNEPH cloud type codes to 3DNEPH cloud type codes via S/R CLDTYP. The heights of the fixed 3DNEPH layers are computed in S/R RTTERR, using as input the ground elevation obtained from S/R RDELEV which reads and unpacks the elevation tape. S/R HTMOD then modifies these 3DNEPH heights to RTNEPH layer heights for the particular cloud distribution present. S/R RDTEMP reads temperatures and heights

of standard pressure levels (via FNOC operational program PNTDAT) and computes temperatures and pressures for the RTNEPH layers. The input data are now in a form in which they can be passed to the Smith-Feddes microphysics portion of the code.

All the input, reading, and processing subroutines are controlled by S/R RDINPT, called by the MAIN segment of the program. After S/R RDINPT returns control to MAIN, S/R FTN75C is called which activates the microphysics portion of the code in the same manner as in the original 3DNEPH program. After microphysics computations are completed and control is returned to MAIN, the output routine S/R WRTOUT, in its modified form, is called to printout results.

The 3DNEPH and single-grid-point RTNEPH models were both run for the ten cloud types covering high, middle, and low clouds (including the convective cloud types, cumulus and cumulonimbus), in numerous combinations of low, middle, and high cloud types for a range of ground elevations (sea level to 2130 m), and with and without precipitation. Comparison of the layer condensed moisture produced by the two models is shown in Figure 1 for all high, middle, and low cloud types except for the convective cloud types. In 72% of the cases (18 of 25), the outputs of the two models match identically, while 88% are within 10% of each other. In those cases where they differ, the differences can be attributed to the greater flexibility with which the RTNEPH model describes the cloud base and cloud top heights, a capability which represents an improvement to the methodology.

The RTNEPH cloud input can produce a different height of the midpoint of the layer (cf. Table 1) which then produces a different midpoint temperature for the layer. If this difference in temperature changes the temperature category in the maximum condensed moisture versus temperature table (Table 2) then the condensed moisture estimate will be different in the two models. This is the situation for all the off-line points except that labeled (L) at the RT value of 0.3 g/m^3 in Figure 1. This point results from the condition described next for convective-type clouds.

In cumulus and cumulonimbus clouds the amount of condensed moisture in a layer is proportional to the percentage which the layer height is of the total depth of the cloud deck. Major differences in condensed moisture can occur between the two model outputs when the height of a particular layer is a larger or smaller percentage of the total cloud deck thickness, as found in the Cb example shown in Figure 2. In

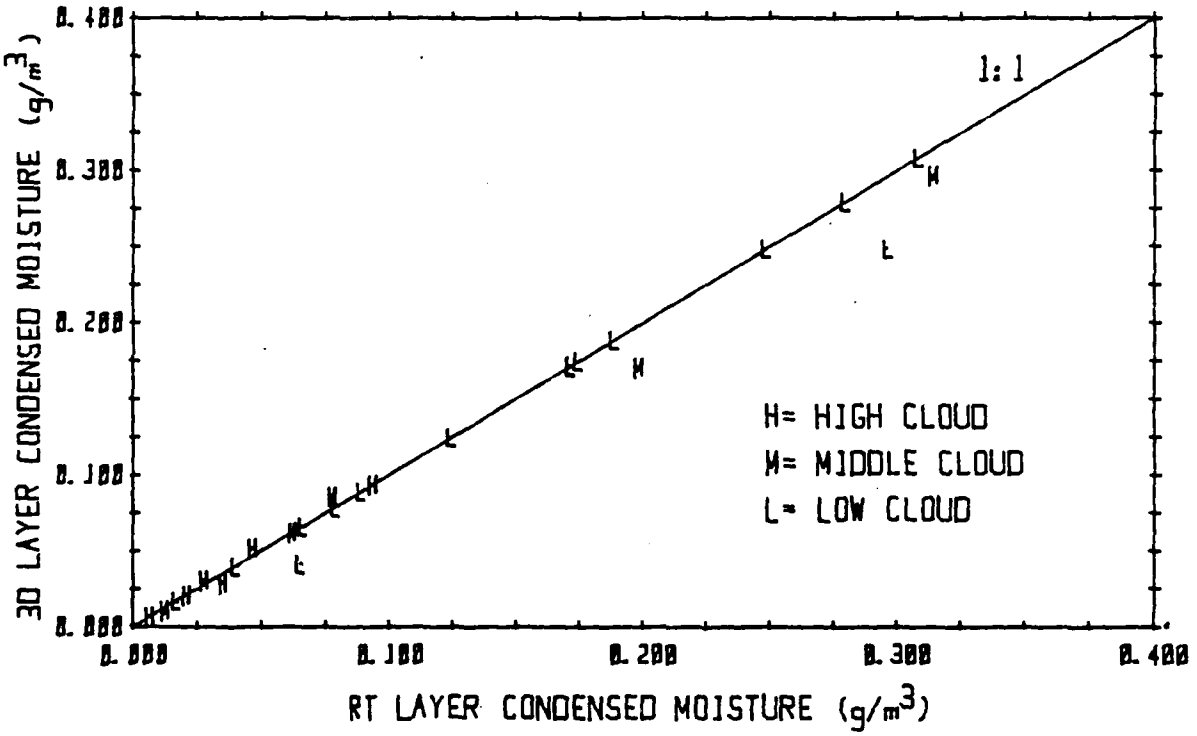

Figure 1 Comparison of Layer Condensed Moisture from 3DNEPH and RTNEPH Smith-Feddes Models for Non Convective Cloud Types.

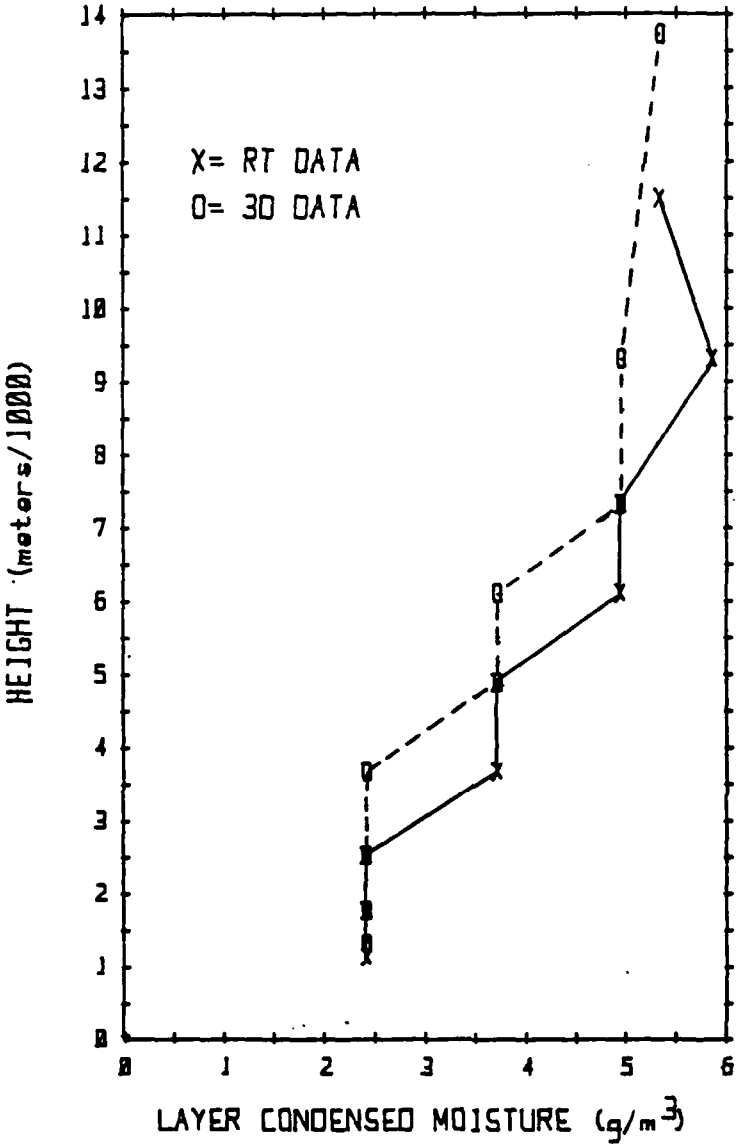

Figure 2 Comparison of Vertical Profiles of Condensed Moisture from 3DNEPH and RTNEPH Smith-Feddes Models for a Cumulonimbus Cloud.

this case, the 3DNEPH cloud deck top is at 16768m while the RTNEPH cloud deck top is at 12300m; the bases of the cloud decks are essentially the same ~ 700m. Major differences between the condensed moisture profiles occur at 3.5 km, 6.0 km and 9.3 km, where the RTNEPH value is larger. In both cases, the RTNEPH layer height is a larger percentage of the total cloud depth. The condensed moisture values are not larger at all heights since in the model the condensed moisture values do not change continuously with height percentage, but rather in a quantum fashion.

A plot of layer condensed moisture for convective type cloud is shown in Figure 3. The agreement between the two models for cumulus clouds is excellent and extends over the entire range of condensed moisture values for cumulus clouds. The numbers beside the data points for cumulonimbus give the total number of observations (more than one) at that moisture value. Eighty-five percent of the total observations essentially fall on the 1:1 line. The values off the line arise from the situation described in Figure 2. Note that three of these points show RT moisture greater than 3D moisture, a result of the more accurate depiction of cumulonimbus cloud top heights in the RTNEPH cloud height data.

In summary, the effort of Task 2 produced an operational Smith-Feddes model at FNOC using RTNEPH cloud data input. The model was coded correctly and operated properly as determined by comparison of results from the scaled-down RTNEPH version with results from the original 3DNEPH version. Any difference between the two model results can be attributed to the RTNEPH cloud data input being a more accurate description of the heights of the cloud decks, compared to the 3DNEPH cloud data input.

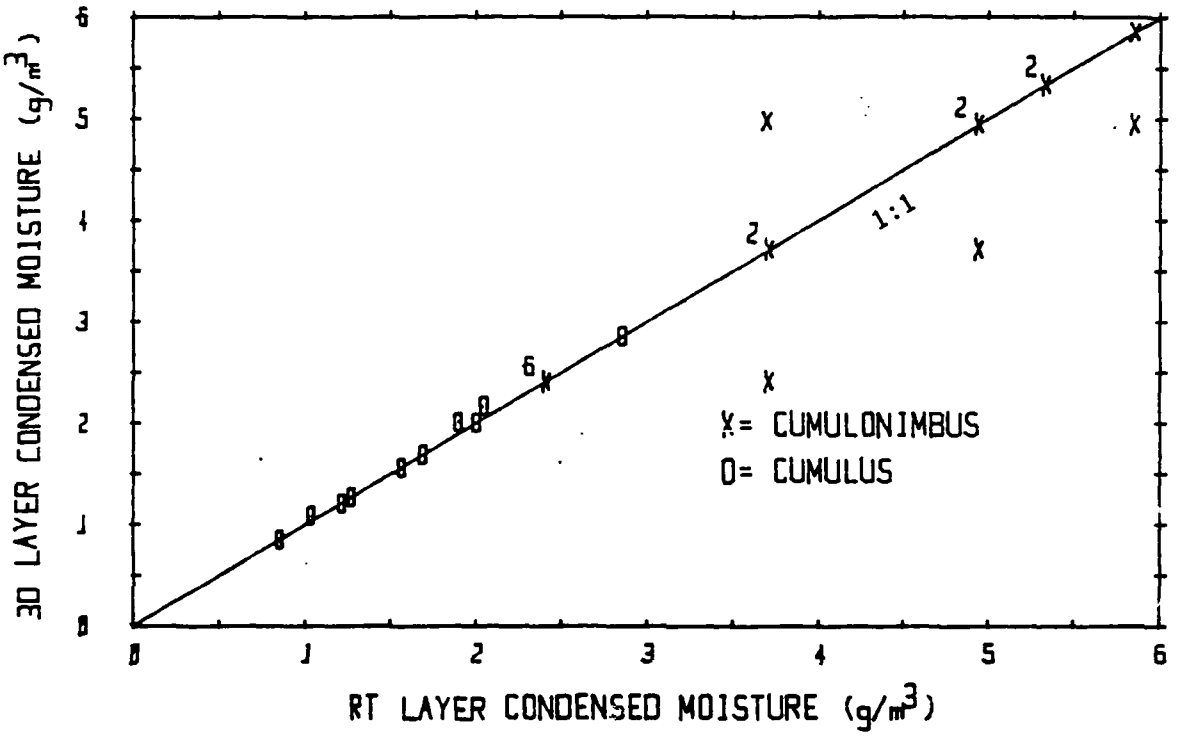

Figure 3 Comparison of Layer Condensed Moisture from 3DNEPH and RTNEPH Smith-Feddes Models for Cumulus and Cumulonimbus.

Section 3

EXAMINATION AND MODIFICATION OF THE SMITH-FEDDES MODEL CLOUD MICROPHYSICS

3.1 INTRODUCTION

Under the Statement of Work Calspan was charged with examining all the cloud physical and thermodynamical parameterizations contained in the SF model. Task 3 was to determine, in light of cloud microphysics observations made during the 10 years since the development of the Smith-Feddes model, whether its microphysics parameterizations should be changed or updated, and, if so, to incorporate any changes into the operational RTNEPH model to be installed and run at FNOC. In particular, we were to examine the specification of condensed moisture, its thermodynamic phase and its subsequent drop size distribution to determine if they were accurate and representative of recent thermodynamic and cloud physical measurements. If it was found that the parameterizations were in error or did not represent current empirical data, they were to be corrected/modified. We performed detailed examinations on all three major components of the S-F model, conducted an extensive review of the literature, and determined the following accuracies and representations of recent thermodynamic and cloud physical measurements.

3.2 SPECIFICATION OF THE MAXIMUM CONDENSED MOISTURE CONTENT IN CLOUDS AS A FUNCTION OF CLOUD TYPE AND TEMPERATURE.

The Smith-Feddes model (Smith, 1974 and Feddes, 1973, 1974) specified the maximum condensed moisture content (CMC) of clouds as a function of their cloud type and temperature. The maximum CMC values, based on observation and theoretical considerations, are presented in Table 2. Documentation of Table 2 was insufficient to determine the origin and validity of each of the reported values, though the basic concept of such a table relating CMC to cloud type and temperature appears to be based on Borovikov (Khrgian, 1963, p. 87-88).

Table 2. Smith-Feddes Look-Up Table of the Maximum Condensed Moisture (in g/m^3) That Can Occur in a Nonprecipitating Cloud as a Function of Cloud Type and Temperature (Feddes, 1973)

Cloud Type	Temperature (degrees C)									
	< -25	-25 to -20	-20 to -15	-15 to -10	-10 to -5	-5 to 0	0 to +5	+5 to +10	+10 to +15	>15
ST	.10	.15	.20	.25	.30	.35	.40	.45	.50	.50
SC	.20	.30	.40	.45	.50	.55	.60	.70	.70	.70
CU	3.0	3.0	3.0	3.0	3.0	3.0	3.0	3.0	3.0	3.0
NS	.35	.40	.45	.50	.60	.60	.75	.90	.90	.90
AC	.25	.30	.35	.40	.40	.45	.60	.70	.70	.70
AS	.15	.20	.25	.30	.30	.35	.40	.50	.50	.50
CS	.15	.15	.15	.20	.20	.20	.25	.25	.25	.25
CI	.10	.10	.10	.10	.15	.15	.15	.20	.20	.20
CC	.05	.05	.05	.05	.10	.10	.10	.15	.15	.15
CB	6.5	6.5	6.5	6.5	6.5	6.5	6.5	6.5	6.5	6.5

The objective of this task was to conduct a literature search and evaluation of recent (~1970 to present) in-cloud measurements of CMC for comparison to the present Smith-Feddes values as given in Table 2. The literature search began with a computer search of nationally archived scientific journal and report data bases. Based on the initial computer search and follow up searches, a data base of 70 recent reports and publications related to in-cloud measurement of CMC was compiled. Additionally, 12 references were gathered for evaluation of the original Smith-Feddes concept and data base. A complete listing of these references is presented in the Bibliography.

Each of the references listed in the Bibliography was evaluated to extract data in the form of maximum CMC as a function of cloud type and temperature. Table 3 indicates which references had data in the cloud type/temperature categories. Preceding the reference number of the entries of Table 3 is the maximum reported CMC for that reference in that category (e.g., the entry for stratus cloud at -25 to -20°C is 0.30-32 indicating that ref. 32 reported a maximum CMC value of 0.30 g/m^3

TABLE 3. The maximum reported CMC (g/m^3) for cloud type and temperature (^oC), with associated reference number, as found in the 1970-1984 literature.

	<-25	-25 -20	-20 -15	-15 -10	-10 -5
St		0.30-32	0.50-32	0.70-32	0.29-21 0.60-32 0.10-28
Sc		0.50-32	0.50-32	0.70-32	0.90-32
Cu			0.60-32	0.56-5 1.5-32 2.9 -51 3.9 -34	3.0-33 2.4-60 1.2-5 3.0-51 1.2-31 1.7-32
Ns	0.13-28	0.17-28	0.43-28 0.42-27 0.43-65	0.20-30 1.7 -28	0.20-30
Ac	0.02-65		0.05-65	1.33-57 0.30-32	0.56-57 0.70-32
As	0.46-28 0.06-27	0.35-28 0.23-27	0.09-21 0.29-28 0.25-27	0.10-21 0.28-27 0.20-32 0.32-28	0.50-32 0.10-27 0.80-28 0.01-26
Cs	0.07-22 0.06-28 0.01-65 0.18-27 0.04-66	0.09-28 0.26-27	0.04-28 0.04-27 0.20-26		
Ci	0.43-22 0.06-65 0.04-66 0.03-43 0.39-26 0.01-65 0.07-27	0.27-26 0.12-27 0.39-22			
Cc	0.01-65 0.08-27				
Cb	0.45-2	2.15-2	0.60-32 6.9 -50 1.1 -3	1.5-32	1.0-32 2.7-13 5.0-33 7.1-50 3.7-15

Table 3. Continued

	-5 0	0 5	5 10	10 15	>15	TEMP NOT GIVEN
St	0.14-21 0.40-28 0.62-58 0.70-32	0.63-21 0.27-58	0.28-62			0.40-19 0.10-40 0.45-11
Sc	1.5-53 1.1-32 0.3-65	0.6-52 0.77-54 0.22-53	0.37-48 0.78-39	0.30-42		
Cu	2.1-36 1.2-37 1.3-32		0.15-35			2.0-38 2.2-6 0.8-68 2.3-10
Ns	0.20-32 1.15-67 0.10-30 0.63-65 0.30-27	0.70-41 0.50-27 0.90-67				0.52-47 0.80-46
Ac	0.50-32					0.16-26
As	0.39-57 0.50-32 0.20-27					
Cs						
Ci						
Cc						
Cb	1.2-32 2.2-3 3.5-18					0.95-26

for that category). Table 3 reveals two important points. First, it delineates where data are available for comparison to Smith-Feddes values. For example, no measurements were found for cirrus clouds at temperatures above -20°C, and only one reference reports data on stratus cloud at temperatures below -10°C. Second, examination of the maximum CMC values shows large, inconsistent variations both within and between the ten cloud type categories. For example, based solely on the maximum for each category, cirrus would be assigned a greater CMC than nimbostratus at temperatures less than -20°C. Also, changes in the maximum CMC for a given cloud type as a function of temperature are often erratic. These large and erratic variations in CMC are attributed to both the sparcity of the data for many of the categories, as well as the fact that while the maximum observed CMC was extracted from each reference, the area of maximum CMC in the cloud may not have been sampled. This was frequently the case for cumulus clouds where often only a single pass through the cloud at a fixed level was performed.

3.2.1 Analysis of CMC data

As discussed above, relatively large, inconsistent variations in the maximum observed CMC values exist in Table 3. Thus to aid in revising the Smith-Feddes CMC values (Table 2), the data from the recent literature were evaluated subjectively, guided by meteorological judgment, with the objective of extracting the maximum CMC value which could reasonably be expected in a given cloud, not necessarily the maximum value ever measured. In this way, momentary "spikes" of large CMC values observed during cloud penetrations were often dismissed in favor of more persistent peak values.

Based on the subjective analysis of the references specified for each cloud type/temperature category in Table 3, maximum expected values of CMC were obtained and are presented in Table 4. A brief summary of the reasoning used to determine the CMC values for each of the cloud types is given below.

Stratus:

In the temperature range of -25 to 0°C, CMC values are based on ref. 32 (taken at the 95 percentile value). Ref. 21 was used for 0 to -5°C temperature interval.

In the 5 to 10°C temperature interval, ref. 62 gives a maximum CMC of approximately 0.28 g/m^3. This value is low compared to what would be expected from ref. 21 and 32 (i.e., ~ 0.5 g/m^3). Since ref. 62 only deals with a single cloud deck (marine stratus off California), the relatively low maximum is attributed to the limited data base and is therefore not considered to be significant, by itself, as a reasonable estimate of the maximum CMC in stratus at that temperature.

Table 4 The Maximum CMC (g/m^3) which can be Expected in Clouds as a Function of Cloud Type and Temperature Based on the 1970-1984 Literature.

	Temperature (°C)								
Cloud Type	< -25	-25 to -20	-20 to -15	-15 to -10	-10 to -5	-5 to 0	0 to +5	+5 to +10	+10 to +15	> 15
ST		0.25	0.30	0.35	0.40	0.45	0.50			
SC		0.40	0.45	0.50	0.55	0.60	0.65	0.70		
Cu				3.0	3.0	2.5				
Ns	(0.30)		(0.45)		(0.75)	(0.70)	(0.50)			
Ac				0.30	0.40	0.45				
As	0.25	0.25	0.25	0.25	0.30	0.40				
Cs	0.15	0.10	0.05							
Ci	0.10	0.10								
Cc	0.05									
Cb	(0.45)	(2.15)	(7.0)	(1.0)	(7.0)	(3.5)				

Stratocumulus:

As with stratus, ref. 32 was the primary reference over the temperature range of -25 to 0°C. Ref. 54 and 39 were used for the temperature intervals of 0 to 5°C and 5 to 10°C, respectively.

Cumulus:

The primary data bases used were from the FACE I (ref. 51), FACE II (ref. 33), and HIPLEX (ref. 60 and 36) cumulus studies. These studies involved the penetration of cumulus clouds at specific temperature levels, ~ -7°C for the FACE programs and ~ -3°C for HIPLEX. The maximum CMC found during these programs was approximately 3 g/m^3 for FACE I, 2 to 5 g/m^3 for FACE II, and 2.5 g/m^3 for HIPLEX.

The analysis of cumulus data was complicated by the large range of vertical development of cumulus clouds ranging from relatively flat cumulus humilis to towering cumulus congestus. Owing to differences in their convective development, these clouds have significantly different CMC's: ~0.5 g/m^3 for cumulus humilis and ~ 5 g/m^3 for cumulus congestus. With respect to the Smith-Feddes model, it would appear unreasonable therefore to classify all cumulus cloud species in the cumulus genus. Therefore, due to their large vertical development, cumulus congestus clouds have been classified in the cumulonimbus genus. Thus, data believed to be from cumulus congestus in the FACE II program (having maximum CMC values of ~5 g/m^3) and data from large cumulus (ref. 16, 47, 15 and 13, having maximum CMC's approaching 4 g/m^3) have been classified as cumulonimbus in Table 2.

The relatively low CMC's reported by ref. 32 and 34A of ~1.5 and 0.15 g/m^3, respectively, are attributed to the limited vertical extent of cumulus clouds comprising these studies.

When examined as a whole, and with the understanding that cumulus congestus clouds have been classified as cumulonimbus, the data from the recent literature generally supports the 3.0 g/m^3 CMC value for cumulus clouds presently specified in the Smith-Feddes model.

Nimbostratus:

Due to the nature of nimbostratus, the presence of precipitation in most of the measurements was unavoidable. As a result, CMC values were often erratic showing relatively high (up to 1.7 g/m^3, ref. 28) peak values. Due to the presence of precipitation in the CMC measurements, as well as the limited number of measurements available, the overall quality of the nimbostratus data base is considered poor. Thus, the values in Table 4 derived from these data are placed in parentheses and, while in

general agreement with the corresponding Smith-Feddes values, probably should not be used to adjust the Smith-Feddes values.

Altocumulus:

Over the temperature range of -15 to 0°C, ref. 57 and 32 were used to obtain maximum CMC values. The values reported in ref. 65 appear low relative to those of ref. 57 and 32 and do not, by themselves, constitute a significant data base.

Altostratus:

In the temperature range of -25 to -10°C, ref. 28 and 27 were used. In the range -10 to -5°C, ref. 32 was used. In the range -5 to 0°C, ref. 57 and 32 were used.

Ref. 28 and 27 both contain clouds which appear to be very deep altostratus with bases at ~ 900 mb and tops extending to ~ 450 mb. Such clouds, which had they been precipitating, would have been classified as nimbostratus, were not considered as representative of altostratus and thus were reclassified as nimbostratus. These clouds had CMC values up to 1.0 g/m^3.

Cirrostratus, Cirrus, and Cirrocumulus:

Data on cirriform clouds were based primarily on ref. 28, 26, 27 and 22. Examination of these references shows CMC measurements ranging from < 0.01 g/m^3 in the cirrus to > 0.40 g/m^3 in cirrus generating cells and precipitation trails. Ref. 26 and 22 concentrated on penetrating dense cirriform clouds, cirrus generating cells, and precipitation trails, and recorded CMC values up to 0.40 g/m^3. While these relatively high values of CMC appear to be free from error, we consider the short-lived types of cirrus penetrated as unrepresentative of widespread cirrus cloud decks reported by RTNEPH. Based primarily on measurements in cirrus fibratus and non-generating cell areas of cirrus uncinus reported in ref. 27, a CMC value of ~ 0.10 at temperatures of $< -20°$ seems reasonable as a maximum expected value.

For cirrostratus, data from ref. 28, 26 and 27 were examined leading to maximum expected values of 0.15, 0.10 and 0.05 for the temperature categories of -25, -25 to -20 and -20 to -15°C, respectively.

Only one cirrocumulus cloud was found in the literature, ref. 27. From the two measurements made in this cloud (one of which may have actually been in cirrostratus or cirrus) a value of 0.05 g/m^3 was obtained.

Cumulonimbus:

The data obtained on cumulonimbus clouds primarily deals with relatively small cumulonimbus/cumulus congestus clouds (ref. 15, 50, 18, 32 and 13) or the anvil caps of cumulonimbus (ref. 2 and 26). Maximum CMC's of 5.1 g/m^3 were reported in ref. 33, values approached 4 g/m^3 in ref. 15 and 18, and a value of ~7 g/m^3 was reported in the precipitation shaft of a cumulonimbus in ref. 50. This data base, however, is not considered sufficiently representative of true cumulonimbus to justify changes of the Smith-Feddes values.

Orographic Clouds:

Ref. 59, 1, 4, 9, 12, 20, 8, 35, 29 and 32 present data on orographic clouds and storms associated with the Sierra Nevada, Cascade, Rocky and Great Dunn Fell Mountains. Due to the strong influence of orography on the cloud physics of such clouds, we do not feel that these clouds should be categorized along with the other entries and, thus, these clouds were not considered in the development of Table 4. Typical maximum CMC reported for these clouds ranged from 1 to 2 g/m^3. Jeck (1983, ref. 32) suggests that orographic clouds formed in air lifted more than ~3 km above ground level could be assigned to the cumulus family.

3.2.2 Conclusion

Based on a comparison of Tables 2 and 4, the subjective assessment of data quality, and the desire to maintain internal consistency, Table 5 presents a revised version of the Smith-Feddes table based on the recent literature. The boxed values are those which differ from the original Smith-Feddes values. A line is drawn under those values where recent data support the original data. The remaining data are the original Smith-Feddes values in categories for which no recent, published measurements were found.

As can be seen in Table 5, only relatively minor adjustments to the original Smith-Feddes table were warranted: values for stratus were all increased by 0.1 g/m^3; values for stratocumulus were, in general, all increased by 0.05 g/m^3; several values for altostratus were increased by 0.05 g/m^3. In general, where recent data existed, they usually supported the existing Smith-Feddes values.

Table 5. Revised Smith-Feddes Table of the Maximum CMC which can be Expected in Clouds as a Function of Cloud Type and Temperature. See Text for Details.

Type	< -25	-25 to -20	-20 to -15	-15 to -10	-10 to -5	-5 to 0	0 to +5	+5 to +10	+10 to +15	> 15
ST	0.20	0.25	0.30	0.35	0.40	0.45	0.50	0.55	0.60	0.60
SC	0.35	0.40	0.45	0.50	0.55	0.60	0.65	0.70	0.70	0.70
Cu	3.0	3.0	3.0	3.0	3.0	3.0	3.0	3.0	3.0	3.0
Ns	0.35	.40	0.45	0.50	0.60	0.60	0.75	0.90	0.90	0.90
Ac	0.25	0.30	0.35	0.40	0.40	0.45	0.60	0.70	0.70	0.70
As	0.20	0.25	0.25	0.30	0.35	0.40	0.45	0.50	0.50	0.50
Cs	0.15	0.15	0.15	0.20	0.20	0.20	0.25	0.25	0.25	0.25
Ci	0.10	0.10	0.10	0.10	0.15	0.15	0.15	0.20	0.20	0.20
Cc	0.05	0.05	0.05	0.05	0.10	0.10	0.10	0.15	0.15	0.15
Cb	6.5	6.5	6.5	6.5	6.5	6.5	6.5	6.5	6.5	6.5

3.3 THE VERTICAL PROFILE OF THE CONDENSED MOISTURE CONTENT OF CLOUDS

Except when specifically noted, the discussion presented in this Section concerns nonprecipitating clouds.

3.3.1 The original Smith-Feddes CMC profiles

Before discussing the CMC profiles found in the recent literature, it is beneficial to first discuss certain aspects of the original Smith-Feddes profiles. Vertical profiles of CMC as used in the Smith-Feddes model are presented in Appendix A. As with the table of maximum CMC's, the documentation for the CMC profiles of the

Smith-Feddes model was insufficient to determine their origin and validity. The lack of documentation makes it difficult to assess the validity of (and recommend changes to) these profiles as the reasoning leading to their specification is unstated.

Two features of the Smith-Feddes profiles appear questionable. First, in none of the profiles does the CMC go to zero at cloud base or top as might be expected from simple adiabatic ascent and diffusion/entrainment considerations. This may be due to a lack of observation at these transitional cloud/clear air zones or perhaps is tied to application and operational considerations specific to the Smith-Feddes model (e.g., in the computer model, cloud CMC is computed at a geometric layer mid-point which by definition never occurs at cloud base or top.) Second, the profiles for St, As, Cs, Ci, Cc, Sc, Ns and Ac, never reach 100% of the maximum expected CMC value. The reasoning behind these profiles is unstated, but it would seem to imply that the values in the Smith-Feddes maximum CMC table were considered too high, at least for application in the Smith-Feddes program.

3.3.2 CMC profiles found in the recent literature

The data base for information on the vertical profile of CMC in clouds is a subset of that used in Section 3.2 to determine the maximum allowed CMC for a given cloud type as a function of temperature. Table 6 indicates the references containing profile information for each cloud type for which data were available. Appendix B tabulates the CMC and cloud height data for each case. Figure 4 presents the CMC profiles for each cloud type (of Table 6) in the manner applicable to the Smith-Feddes model, i.e., as percent of maximum condensed moisture vs. percent height above cloud base. The CMC profiles for each cloud type are summarized in Table 6 which presents the average percent height above cloud base at which the maximum CMC was observed. Also tabulated are the corresponding Smith-Feddes model values.

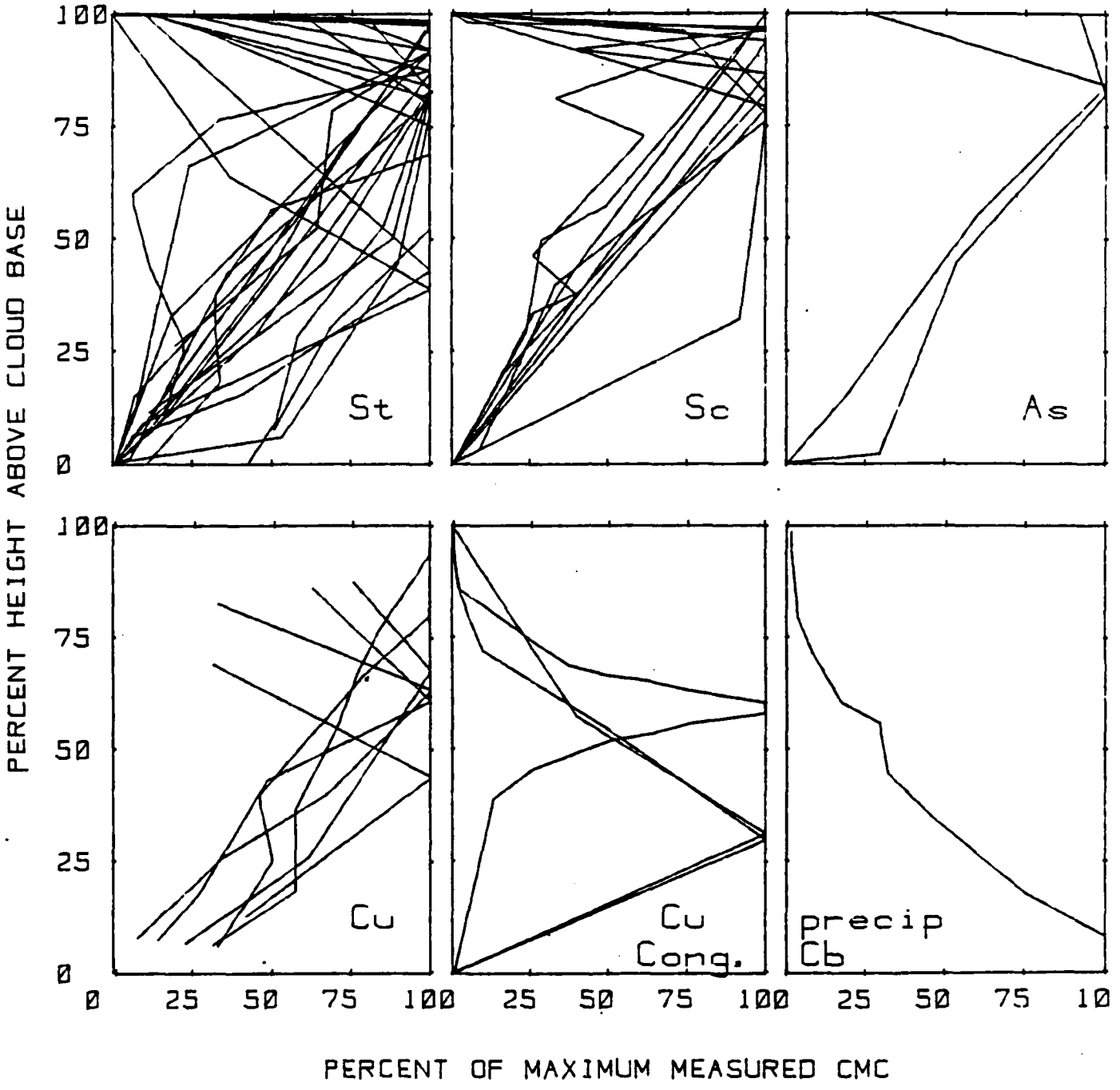

FIGURE 4 Observed vertical CMC profiles found in the recent literature for the cloud types indicated.

Table 6. Summary of References Providing Cloud CMC Vertical Profile Data

Cloud Type	Reference No.	Height of Maximum CMC in Percent of Cloud Depth: Recent Literature	Height of Maximum CMC in Percent of Cloud Depth: Smith-Feddes Model
Stratus	21, 58, 62	81%	Constant
Stratocumulus	52, 54, 48, 42, 53	89%	50%
Altostratus	21	83%	Constant
Cumulus	10	69%	73%
Cumulus Congestus	18	59%	75%
Precipitating Cu	28	0%	0%

Examination of the CMC profiles for stratus, stratocumulus, altostratus and cumulus suggests that the CMC profile can be modeled as linearly increasing from 0% of the maximum CMC at cloud base to 100% at heights generally ranging from ~75 to 95% above cloud base, followed by a linear decrease to 0% at cloud top. The profiles for cumulus congestus are from different areas of a single cloud--i.e., the updraft, core and downdraft regions--with the core profile having maximum CMC at ~60% height above cloud base. The precipitating cumulus profile shows a maximum CMC at cloud base, with CMC decreasing with height. In the case of stratus, altostratus and cirrus, the Smith-Feddes model indicates no variation of CMC with height.

Based on Figure 4 and the summary given in Table 6, the following conclusions and preliminary recommendations are made:

1. The vertical profiles of CMC in stratus, stratocumulus, and altostratus are similar and can all be modeled as linearly increasing from 0% of this maximum CMC at cloud base to 100% of the maximum CMC at a height of 85% above cloud base, followed by a linear decrease to 0% of the maximum CMC at cloud top. It is recommended, therefore, that the Smith-Feddes profiles for these cloud types (St, Sc, As) be changed to reflect this general profile.

2. The profile of CMC in cumulus increases linearly from 0% of the maximum CMC at cloud base to 100% of the maximum CMC at a height of 70% above cloud base, followed by a linear decrease to 0% of the maximum CMC at cloud top.

The percent height above cloud base of maximum CMC for cumuli is consistent with the Smith-Feddes model (69% vs. 73%). However, the Smith-Feddes CMC profile does not go to zero at cloud base and cloud top. As can be seen in Figure 4, the profiles shown do not extend to cloud base or cloud top (in each case, the cumulus cloud was penetrated at three to six specific levels) though the CMC values rapidly decrease as cloud base and top are approached. It is recommended, therefore, that consideration be given to changing the Smith-Feddes profile for cumulus to show zero CMC at cloud base and top.

3. The CMC profiles for cumulus congestus differ from the Smith-Feddes profile for cumulus and cumulonimbus but are not sufficient evidence to change the Smith-Feddes profile. More data are required to assess this category.

4. The CMC profile for the precipitating cumulus is consistent with the corresponding Smith-Feddes profile.

5. For cloud types for which vertical CMC profiles were not found in the recent literature (i.e., Ns, Ac, Ci, Cc, Cs, Cb), it is suggested that CMC profiles for these cloud types be assigned as follows:

- Ns and Ac: assign profile as described in (1) above.
- Cb: assign profile as described in (2) above for Cu.
- Ci, Cs and Cc: Lacking any CMC profile measurements for these clouds, the Smith-Feddes model profiles could be retained. However, the justification for nonzero CMC values at cloud top and base, and the failure of the profile to reach 100% of the expected CMC value, as discussed in Section 3.3.1, should be examined.

3.4 ALTERNATIVE PROCEDURE FOR SPECIFICATION OF THE CONDENSED MOISTURE CONTENT OF CLOUDS

3.4.1 Problems with the Smith-Feddes Procedure for Specifying CMC

In the course of evaluating the recent literature for CMC data to compare to the Smith-Feddes model, two points surfaced which suggest that the present procedure of specifying CMC based on cloud type and temperature may be inappropriate. First, the nonuse of cloud depth information to aid in determining CMC appears to result from a misapplication of the original development by Borovikov (in Khrgian, 1963) of the temperature dependence of cloud water content, upon which the Smith-Feddes model appears to be heavily based. The second point deals with the inability of the ten basic cloud types to adequately define the magnitude of the CMC of clouds within a given cloud type. These two points are discussed below.

- Dependence of Cloud Water Content on Temperature and Cloud Depth

Borovikov begins his discussion on the temperature dependence of cloud CMC by discussing the adiabatic process and presents a relation to compute the adiabatic CMC of clouds. In this relation, cloud CMC is a function of the cloud depth, adiabatic temperature lapse rate, and the rate of change of specific humidity with temperature. By assuming cloud depth to be constant within a given cloud genus, the expression is reduced, making cloud CMC dependent only upon a constant and the rate of change of specific humidity with temperature. The constant cloud depth assumption is reasonable only when dealing with clouds of similar depth as appears to be the case for Borovikov's study. However, the use of Borovikov's results on a world-wide basis, as in the application of the Smith-Feddes model, seems to be an oversimplification in view of the significant differences in cloud depth which may occur between various cloud species of a given genus, as well as the general difference in cloud depth between tropical, temperate, and polar regions. Furthermore, the assumption of a constant cloud depth would appear unnecessary since the input data to the Smith-Feddes model contains cloud depth information.

Having made the assumption of a constant cloud depth for a given genus, the maximum values of CMC as a function of temperature derived from observations frequently come from the thicker clouds sampled. The stratus, stratocumulus, and

cumulus data examined in the literature search (Section 3.2 and 3.3) clearly show this was the case. Thus the deduced values overestimate the CMC of less thick clouds; and similarly, values may be underestimated in unusually thick clouds.

To demonstrate the significance of cloud depth on the maximum CMC, data from the vertical CMC profiles for stratus, stratocumulus, altostratus and cumulus are presented in Figure 5 in terms of the maximum measured cloud CMC vs. cloud thickness. As can be seen, there is a definite increase in CMC with greater cloud depth.

- The Relationship of Cloud Genera to CMC

It became apparent during the literature evaluation that the ten basic cloud genera (St, Sc, Su, Ns, Ac, As, Cs, Ci, Cc, Cb) do not adequately define the CMC for all cloud species within a given genus, possibly because the origin of the genus classifications were not based on cloud CMC but rather on cloud macrostructure, cloud base height, and convective activity. Hence, significant variations in cloud CMC can occur between cloud species of the same genus. For example, in the cumulus genus, the cumulus humilis cloud has limited vertical extent and CMC of ~ 0.5 g/m^3 while the cumulus congestus cloud has great vertical extent and large CMC of ~ 5 g/m^3. (This example also demonstrates the dependence of CMC on cloud depth as discussed above.)

Thus, based on the problem of cloud genera not being adequate to define the CMC of the various cloud species of a given genus and the implied use of the oversimplifying assumption of a constant cloud depth for all clouds of a given genus, it is recommended that alternative procedures for defining cloud CMC be investigated.

3.4.2 An Alternative Technique to Specify Cloud CMC

While gathering data on the vertical distribution of cloud CMC, it was apparent that these profiles could often be closely approximated by the adiabatic CMC profile or, at least, presented as some fraction of the adiabatic profile. For several of the vertical profiles presented in Section 3.3, the adiabatic profile was also provided for comparison (see ref. 52, 54, 42, 53, 18 39 and 62). In general, stratus and stratocumulus clouds closely followed the adiabatic profile. For cumulus clouds, due to entrainment, the observed profiles were generally less than the adiabatic profiles, though the CMC profile could still be represented as a function of the adiabatic profile. Figures 6, 7 and 8 present examples of observed and adiabatic profiles for stratus, stratocumulus and cumulus, respectively, excerpted from the literature.

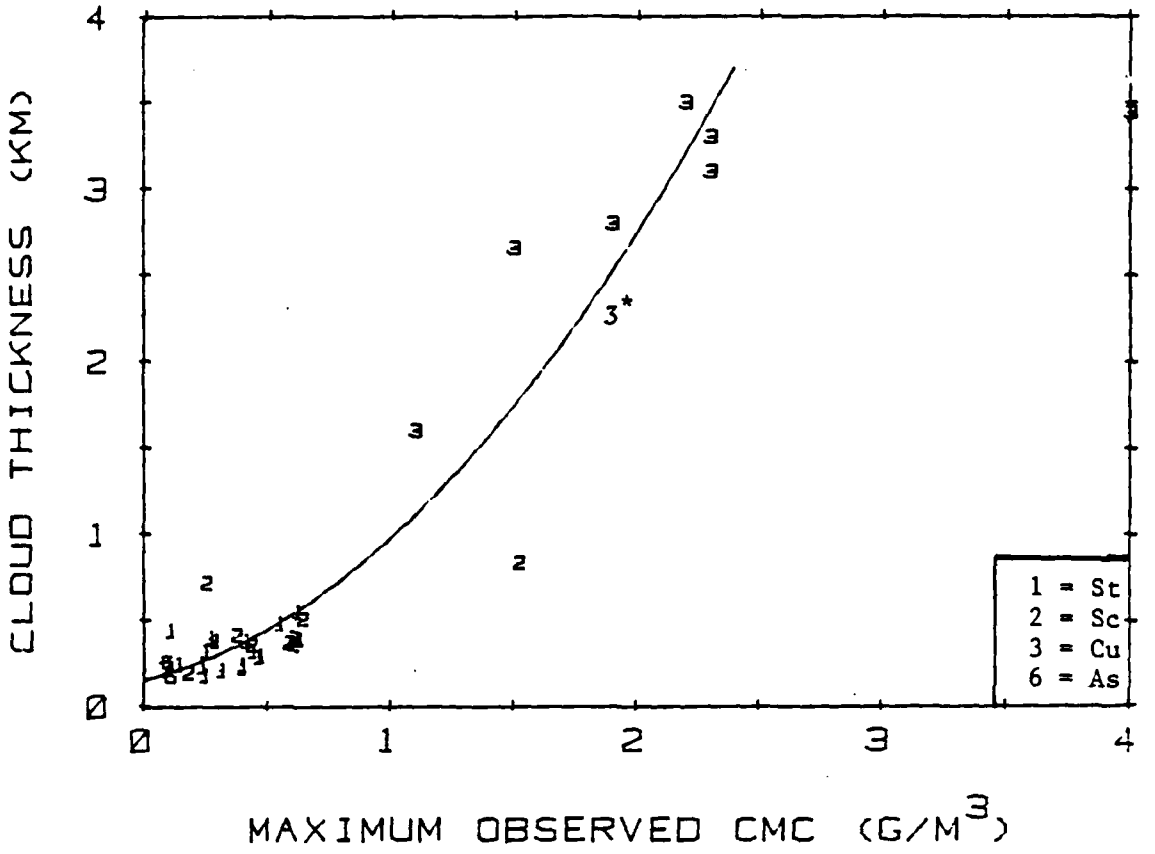

*A.M. Blyth and J. Latham,1985: "An Airborne Study of Vertical Structure and Microphysical Variability Within a Small Cumulus," Quart. J.R. Met. Soc.,111,pp. 773-792.

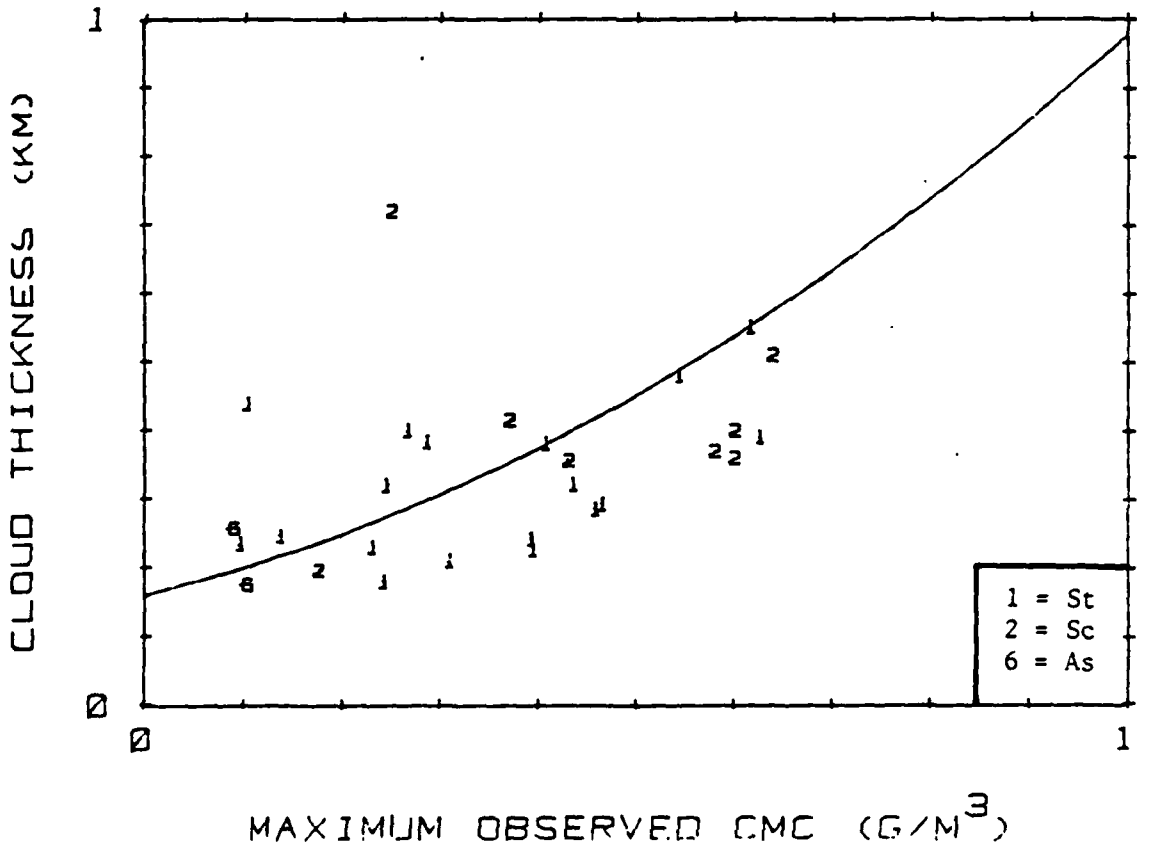

FIGURE 5 Maximum reported cloud CMC versus cloud depth.

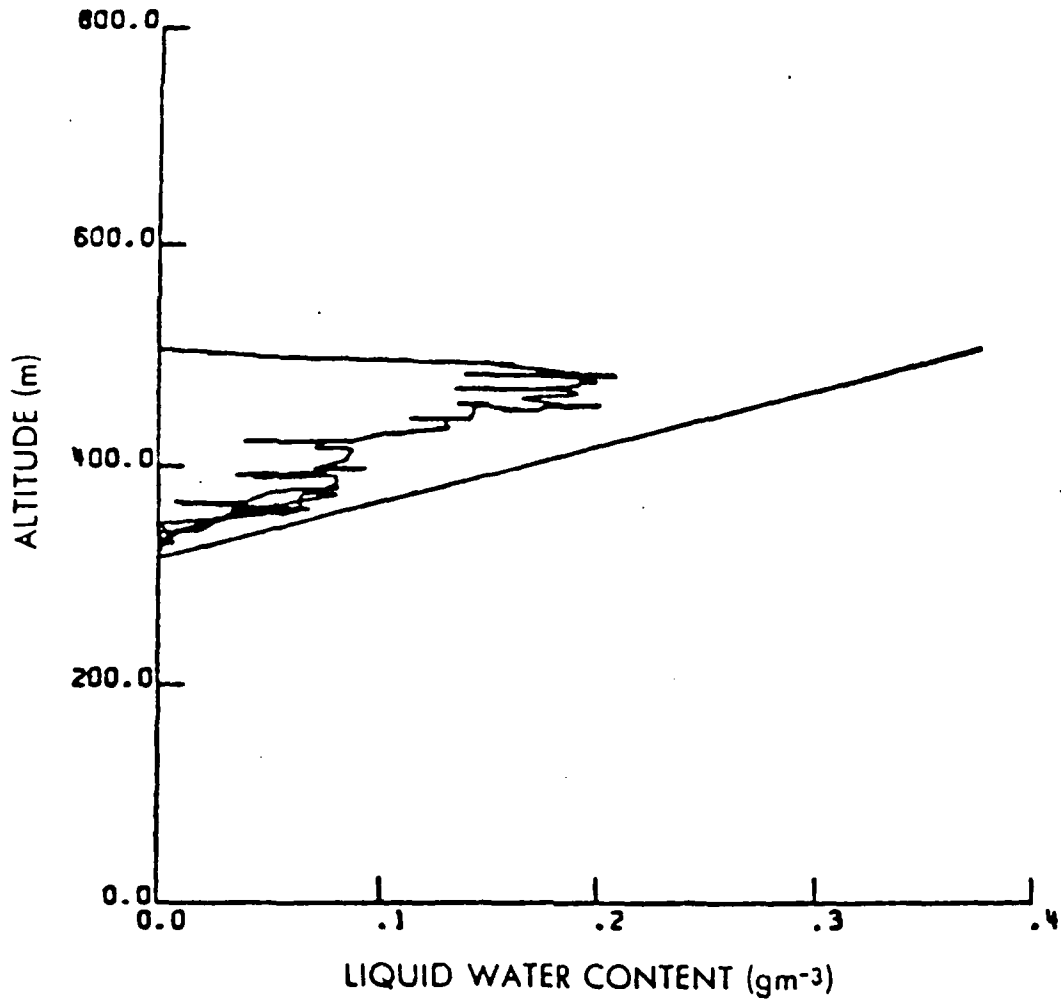

FIGURE 6 Observed and adiabatic (straight line) vertical CMC profile in stratus cloud (Ref 62).

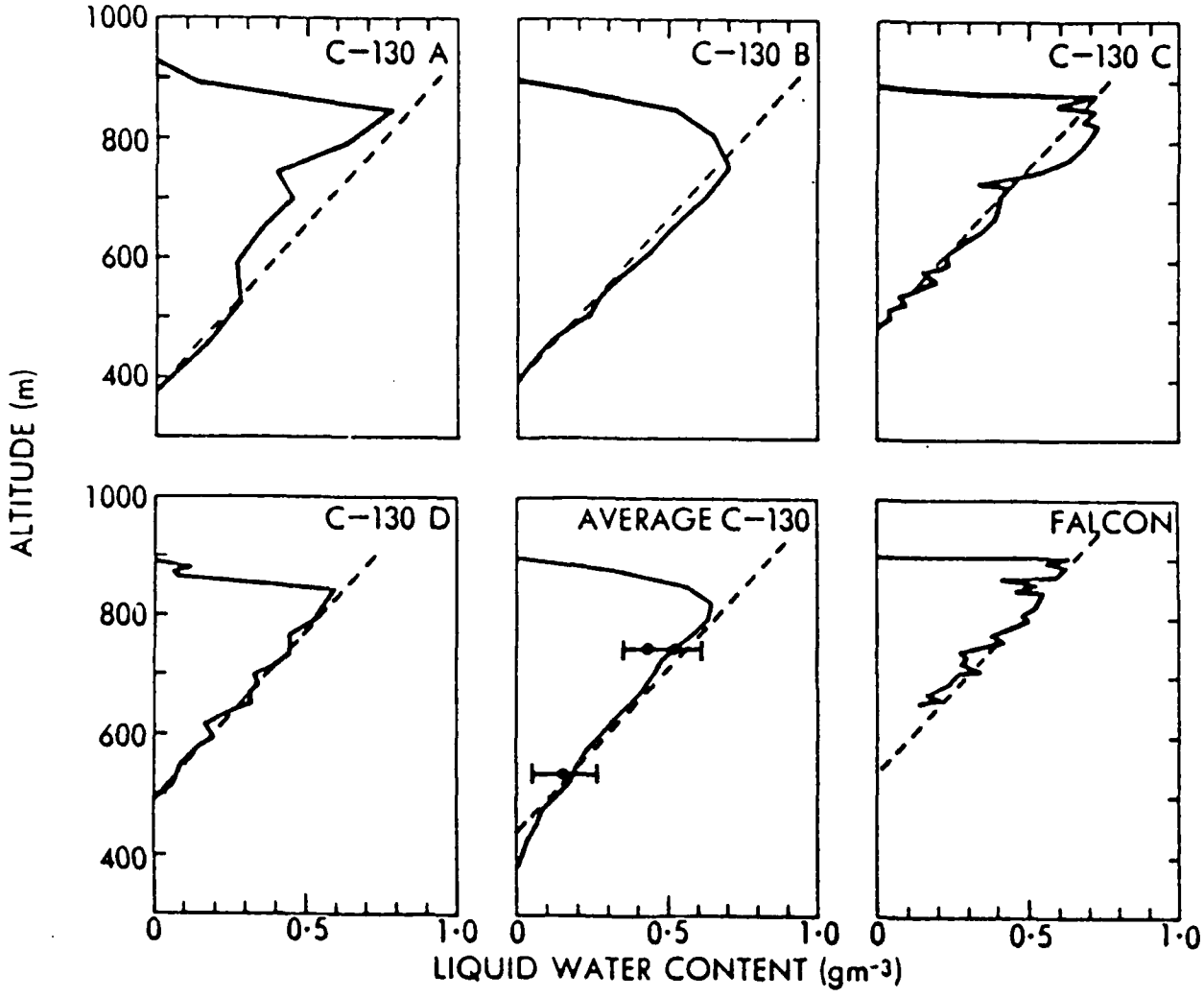

FIGURE 7 Observed and adiabatic (dashed line) vertical CMC profiles in stratocumulus (Ref 54).

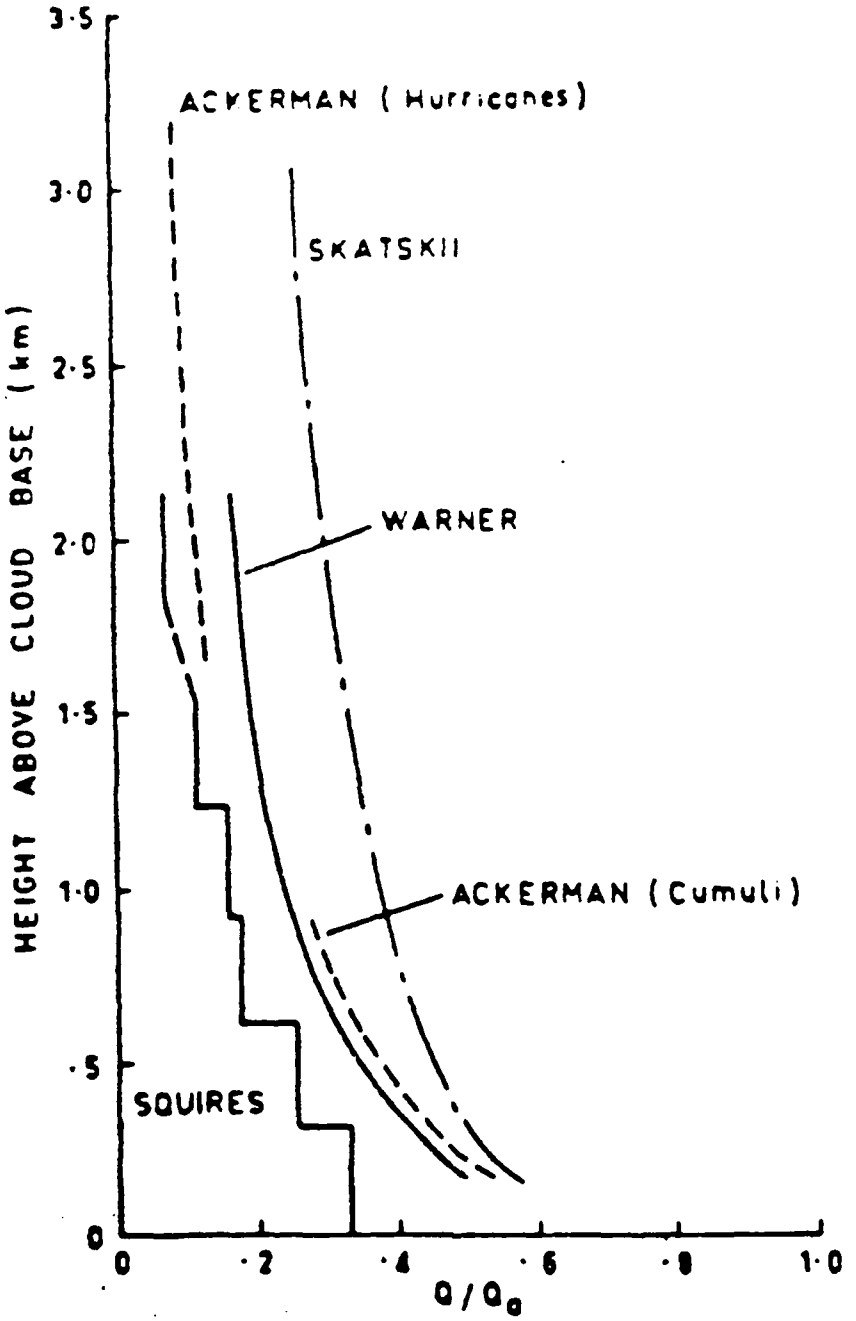

FIGURE 8 Vertical profile of the ratio of the observed mean CMC to the adiabatic value in cumulus cloud (Ref 61).

A method of specifying the CMC of clouds based on the adiabatic CMC profile would take full advantage of the cloud depth and temperature data available to the Smith-Feddes model. Where appropriate, the adiabatic profile could be modified based on the cloud genus information (e.g., to compensate for entrainment in cumulus). The procedure would eliminate the look up table of maximum CMC as a function of cloud type and temperature, and would replace the CMC profiles by adiabatic profiles or modified adiabatic profiles in a format similar to that presented in Figure 8.

Clearly, the adiabatic profile is not applicable to precipitating clouds, and hence the Smith-Feddes model profiles in precipitating clouds should be retained.

3.5 ADIABATIC COMPUTATION OF CMC

After consultation with the COTR, it was decided to implement the adiabatic generation of CMC in the S-F model. Starting at cloud base, the computer code (1) calculates the moist adiabatic lapse rate of temperature, (2) computes the moist adiabatic temperature at a level 100m above the cloud base, (3) computes the saturation vapor density with respect to water, ρ_w, at the upper level, and (4) computes the CMC at the upper level as the difference between the lower and upper values of ρ_w. This procedure is repeated until the CMC at the mid-point of the S-F geometric cloud layer is computed. This midpoint value of CMC is then transferred to the microphysics portion of the S-F computer program. If a cloud deck encompasses more than one geometric layer, the above procedure is repeated until a CMC is calculated at the midpoint of all the layers.

3.5.1 Computation of Liquid Water Generated During Saturated Adiabatic Ascent

The computation of liquid water generated during adiabatic ascent proceeds by:

1) computing the saturated adiabatic lapse rate at a height, z

2) computing a temperature at a higher height ($z+\Delta z$) based on this lapse rate

3) computing a new saturation vapor density, ρ_w at this new temperature

4) computing the liquid water generated over Δz as the difference between ρ_w at z and ρ_w at $(z+\Delta z)$.

The equation used for saturated adiabatic lapse rate is Eq. (19.2) from Haurwitz (1941)

$$\frac{dT}{dz} = -g \left[\frac{1 + 0.621 \frac{e_s}{p} \frac{L}{RT}}{Cp + 0.621 \frac{L}{p} \frac{de_s}{dT}} \right] \quad 1)$$

where T = ^oK and Haurwitz's A (reciprocal of mechanical equivalent of heat) is set equal to one since R and Cp are in the same units.

In this equation,

e_s = saturation vapor pressure of water
p = total atmospheric pressure
R = gas constant for dry air = .06855 cal/gm (air) -deg
Cp = specific heat at constant pressure for dry air = 0.239 cal/gm (air)-deg
L = heat of vaporization for water = 595. - 0.5t(^oC) (cal/gm-(water))
t = ^oC
g = acceleration of gravity = 980 cm/sec^2.

Saturation vapor pressure of water is obtained from Bolton (1980) (Eq. 10):

$$e_s = 6.112 \exp \left[\frac{17.67t}{t+243.5} \right] \quad 2)$$

while $\frac{de_s}{dT}$ is obtained by differentiation of 2).

In the S-F computer program Eq. 1) is evaluated every 100m starting at the observed cloud base; and liquid water content is also computed every 100m with

ERRATA - UPDATING THE SMITH-FEDDES MODEL

Calspan Report No. 7330-1

C. William Rogers
James T. Hanley
Eugene J. Mack

Section 3.5.1 Computation of Liquid Water Generated During Saturated Adiabatic Ascent

Steps 3 and 4 should read:

"3.) computing a new mixing ratio, r_w at this new temperature.

4.) computing the liquid water generated over ΔZ as the difference between r_w at Z and r_w at $(Z+\Delta Z)$. This difference is converted to g/m^3 by multiplying by the mean density over ΔZ."

The discussion in Section 3.5.2, which is based on liquid water content as the difference in water vapor density over ΔZ, is still valid when the difference in mixing ratio over ΔZ is used, although the adiabatically computed CMCA's will be smaller.

LWC set equal to zero at cloud base. This procedure is repeated until the CMC (LWC) at the mid-point of the S-F geometric cloud layer is computed. This midpoint value of adiabatic CMC (CMCA) is then transferred to the microphysics portion of the S-F computer program. If a cloud deck encompasses more than one geometric layer, the above procedure is repeated until a CMC is calculated at the midpoint of each successively higher layer.

3.5.2 Reduction of CMCA due to Entrainment

The reduction of adiabatic CMC (CMCA) due to entrainment in convective clouds is based on data published in Warner (1970, Fig. 1), Fig. 8. After examining Warner's discussion of the various profiles in Fig. 8, we decided to use the curve labeled 'Warner'. This curve was extrapolated downward to CMC/CMCA (Q/Q_a) equal to 1.0 at cloud base. Meteorological experience and judgment led to establishing a minimum CMC/CMCA value of 0.2 and therefore constant CMC/CMCA ratio above 1.5 km above cloud base. If

$$\text{CMC/CMCA} = az + b \qquad 3)$$

where z = height above cloud base, then the values used for the various height layers above cloud base are shown in Table 7.

Table 7 Parameters for CMC/CMCA ratio (Eq. 3) as a function of height above cloud base.

Height above cloud base (m)	a	b
0-32	-1.1E-2	1.0
33-177	-1.4E-3	0.6915
178-726	-3.56E-4	0.505
1500	0.0	0.2

These CMC/CMCA reductions were tested on observations of cumulus and cumulonimbus clouds contained in the RTNEPH test tape. The resulting CMC values are shown in Table 8 along with the original S-F values from the CMC vs. temperature table (Table 2).

Table 8 Comparison of Adiabatic CMC and S-F Tabular CMC for Observed Cumulus and Cumulonimbus Clouds.

	Cumulus	
Height Above Cloud Base (m)	Adiabatic CMC (g/m^3)	S-F Tabular CMC (g/m^3)
212	.119	1.2
653	.213	1.8
1376	.289	2.85

	Cumulonimbus	
Height Above Cloud Base (m)	Adiabatic CMC (g/m^3)	S-F Tabular CMC (g/m^3)
412	.579	2.405
1053	.884	2.405
1816	1.251	2.405
2959	1.830	3.705
4178	2.30	3.705
5398	2.639	4.94
6617	2.867	4.94
8600	3.058	5.85
10786	3.117	5.33

The more realistic adiabatic CMC, over the tabular S-F CMC for both cloud types, is clearly evident from the table; e.g. the smaller values in the lower levels of the cloud and the overall more reasonable values within the rest of the cloud.

Initially, no reduction from CMCA for the other two convective cloud types, Sc and Ac, was planned. However, when tests were run on observations of these cloud types on the RTNEPH test tape, extremely large CMCA values were produced. Therefore it was decided to reduce the CMCA values for Sc and Ac in the same fashion as was done for Cu and Cb. The resultant CMC and CMCA values and S-F tabular values are shown in Table 9. It is readily apparent that a reduction in CMCA values

to account for entrainment processes is also required for the Sc and Ac cloud types to bring them closer to observed values (e.g., S-F tabular CMC data).

Table 9 CMCA and S-F Tabular Values for Ac and Sc

Cloud	Height above Cloud Base (m)	CMCA (g/m^3)	Reduced CMCA (g/m^3)	S-F Tabular CMC (g/m^3)
Sc	724	1.266	.476	.433
Sc	1181	3.140	.732	.520
Ac	1767	2.110	.510	.445

For the stratiform cloud, it was decided to use the purely adiabatic CMC with no reduction for entrainment. Data support adiabatic CMC profiles in altostratus (Ref. 57) and stratus (Ref. 13). Values of CMCA along with S-F tabular values for observation of these cloud types from the RTNEPH test tape are shown in Table 10.

Table 10 CMCA and S-F Tabular CMC Values for St, As, and Ns

Cloud	Height Above Cloud Base (m)	CMCA (g/m^3	S-F Tabular CMC (g/m^3)
St	100	.212	.160
As	500	.548	.120
Ns	900	1.007	.369

For the thicker cloud, the adiabatic values are larger than the tabular values, but also probably more realistic, especially for the Ns where a 1 g/m^3 CMCA is more representative of a precipitating cloud than the S-F tabular value of 0.37 g/m^3.

In order to incorporate cloud depth information into the specification of CMC, the S-F model now computes CMC via the moist adiabatic process. St, Ns, and As use 100% of the adiabatic vlaue, while cumuliform clouds (Cu, Cb, Sc and Ac) use a value reduced to account for entrainment (after Warner, 1970). CMC for cirriform (ice) clouds is still specified from the Smith-Feddes table (Table 5).

3.6 DROP SIZE DISTRIBUTIONS

In the Smith-Feddes model, the cloud drop size distribution is computed from a parameterized equation which is based on the concept of dividing the fraction of total liquid water content present in a given drop size interval by the mass of a single droplet of that size, thereby obtaining a droplet number concentration. A major input to the drop concentration equation is the condensed water content obtained from the water content versus temperature table discussed in Section 3.2. Microphysics input parameters in the equation are values of the mode of the drop size distribution and the percentage of condensed water content at the mode, both as functions of cloud type. These parameterizations appear to have been derived (Feddes, 1974; Smith, 1974) primarily from liquid water content distributions published by Diem (1948) and reproduced by Mason (1957, 1971). These data are relative distributions, since the LWC distributions as functions of droplet size are in arbitrary units.

3.6.1 Cloud Drop-size Distributions

The drop-size distributions in the S-F model are produced from an equation which for each cloud type requires the parameters: (1) mode droplet size, (2) the fraction of liquid water content which occurs at the mode, and (3) the mass of the droplet at the mode. An initial examination of the S-F mode radii revealed that many of the values were small relative to observed values. In order to examine this discrepancy, we attempted to duplicate those S-F parameters which were derived from cloud microphysics measurements, i.e, parameters (1) and (2) above.

A way to compute these parameters is to determine the distribution of the fraction of total LWC as a function of droplet size. The relative drop size distribution is then obtained by dividing the fractional LWC's by the mass of the appropriately sized droplet. The droplet mode then follows by inspection. This procedure is essentially that outlined by Feddes (1974, p. 7 and 11-12).

The basic question is: What cloud microphysics observations were used by S-F to obtain the distribution of fractional LWC? Smith (1974) definitely indicated that the relative LWC distribution vs. droplet size curves of Diem (1948), as reproduced in Mason (1971), were used (Fig. 15, p. 17, Smith (1974)). These curves are reproduced here in Fig. 9.

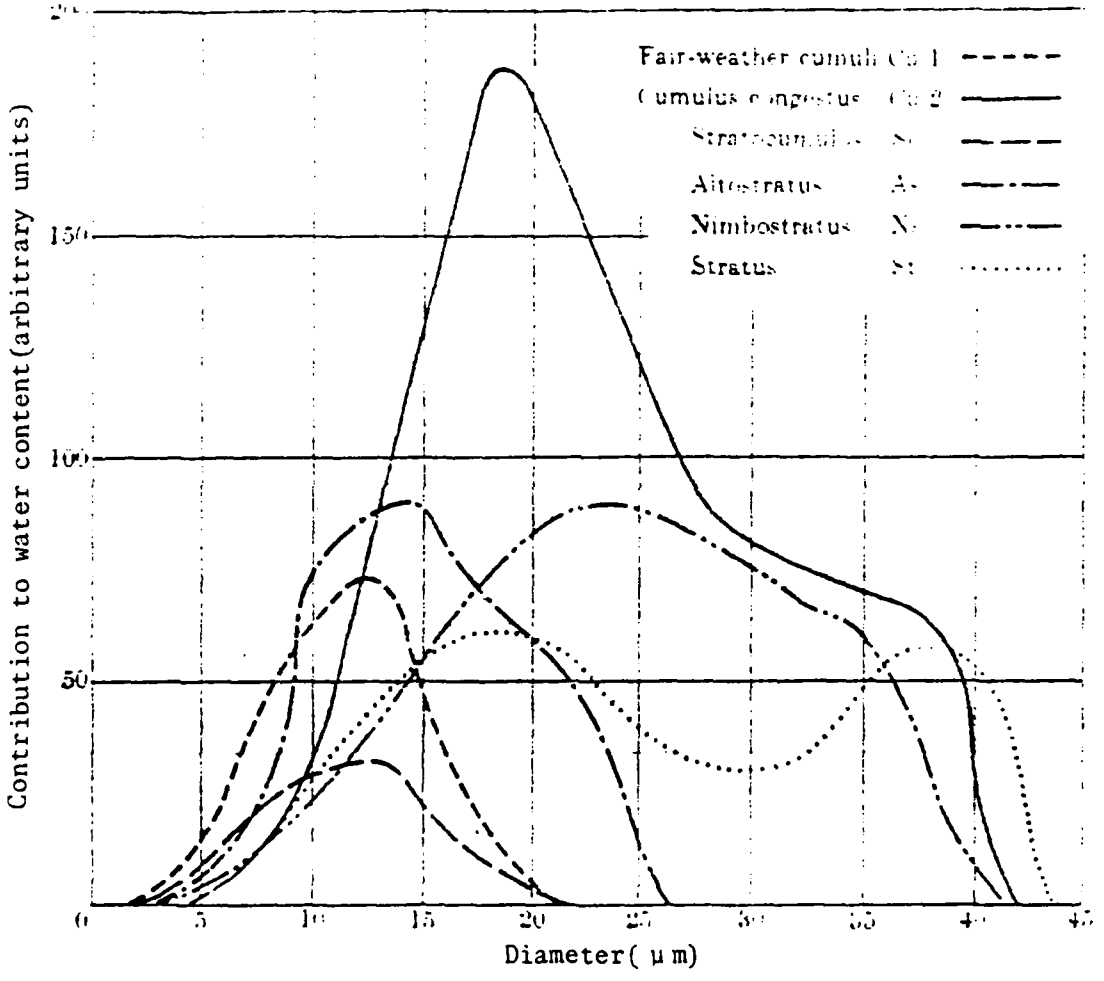

Figure 9. The Contribution made by droplets of various sizes to the liquid water content of different types of cloud. (From Diem(1948)),(From Mason(1971)).

The procedure we used to analyze these curves was as follows:

1. Digitize the curves at one micron intervals;

2. Sum up the individual digitized values to obtain their total;

3. Compute the corresponding fractional LWC at one micron intervals.

The relative drop size distribution was then obtained by the Feddes procedure as outlined above. The mode radii we obtained through this analysis and those used in the S-F model are shown in Table 11.

Table 11 Comparison of drop size distribution mode used in S-F model and Calspan-computed values from Diem's (1948) relative liquid water content distributions, radius (μ m).

CLOUD TYPE	S-F MODEL	CALSPAN COMPUTED
	Mode Radius	Mode Radius
St	2.5 μ m	8.5 μ m
As	7.5	3.5, 9.5
Ns	2.5	3.5
Cu	2.5	2.5
Sc	2.5	2.5
*Cb	10.0	13.5
Ac	2.5	**

* Smith-Feddes provides parameterizations for cumulonimbus (Cb), while Diem has data for cumulus congestus but not for (Cb). Since these cloud types are closely related, in the following discussion we shall merge data from both cloud types into one cloud type, Cb.

** Altocumulus cloud is not present in Diem's data.

Except for stratus, the S-F and Calspan values generally match. The S-F altostratus value is approximately an average of the two Calspan-derived peaks, while the others

are fairly close. The foregoing analysis suggests that Diem's LWC curves were used to obtain the S-F mode values. However, these values do not match observations.

Consider the data presented in Table 12 which provides S-F modes along with various measurements of mode from a table in Mason (1971) and from recent observations.

Table 12 Comparison of drop size distribution modes used in S-F model and observed modes, radius (μm)

	Mode Radius		
Cloud Type	SF Model	Mason Table (1971)	Recent Observations
St	2.5 μm	4 μm	3-4 μm
			1.5-3
			5-7
As	7.5	4.5	-
Ns	2.5	4	7-10
Cu	2.5	4-11	5-10
Sc	2.5	3.5	5-10
Cb	10.0	5.5	7

Compared to the observed values, the As and Cb S-F values are too high, while for the other cloud types the S-F values are too low. The S-F Cu and Ns values are not supported by any observations. The S-F Sc value is not supported by recent measurements, while the St value seems representative only of recent measurements in Arctic stratus.

An analysis indicated that the digitization of the Diem LWC curves may have been the source of shifting the peaks to the incorrect lower values. As seen in Fig. 9, below 5 μm the curves all have small values near zero, and thus it is easy to make errors in extracting digital values. Errors in LWC at these small radii can cause large errors in drop concentration when the fractional LWC is divided by the mass of the drop. In fact the error could be large enough so as to shift the mode in the calculated drop concentration to these small sizes, e.g. to around 2.5 μm as seen in Table 11.

To test this explanation we alternately computed the LWC fraction per interval (LWC_i) from Diem's companion relative drop size distributions which were also published in Mason (1971). The equation used was

$$LWC_i = \frac{N\ 4/3\ \pi\ r_i^3\ f_i}{N\ 4/3\ \Sigma\pi r_i^3\ f_i} \qquad \text{Eq. 4)}$$

where:

N = total number of drops

r_i = radius at center of one micron interval

and f_i is the fraction of drops per one micron interval

Then for each S-F mode radius in Table 11, the above computed LWC_i was converted to a digitized value of relative LWC. This conversion was done by multiplying the appropriate LWC_i from Eq. 4) by the sum of values obtained in the digitization of the LWC curves in Fig. 9. In this way we computed relative LWC values based on the drop-size curves for comparison with the values digitized from the LWC curves. The results are shown in Table 13.

Table 13 Comparison of Calspan extracted relative LWC value at S-F mode (Fig. 9) and Calspan computed LWC (at S-F mode) using relative drop distribution. (Arbitrary units, see Fig. 9).

Cloud Type	S-F Mode (radius μm)	Calspan Extracted Relative LWC value at S-F Mode (Fig. 9)	Calspan Computed LWC Value (At S-F Mode) using Relative Drop Distribution
St	2.5 μm	1 (Arbitrary Units)	0.7 (Arbitary Units)
Ns	2.5	2	0.6
As	7.5	4	0.5 (3.5 Peak)
Cu	2.5	4	0.26
Sc	2.5	2	0.20
Cb	10.0	98	82

First notice that all the digitized LWC values are larger than the corresponding values calculated from the dropsize distributions. The larger digitized values of LWC lead to larger number concentrations, larger by so much that (for all clouds except Cb) the modes are shifted to smaller sizes relative to observed mode sizes. The reason for the larger digitized values lies apparently in the fact that at the scale used in the Diem plots the curves cannot be plotted or digitized accurately below 5 microns. In addition the curves for individual cloud types merge in this region presenting further complexity to digitization.

The radii at which the peaks in drop concentration are parameterized in the S-F model are incorrect, and consequently the fractional LWC at the peak are also incorrect. This conclusion has been demonstrated above from Diem's data for cloud types St, As, Ns, Cu, and Sc. Diem has no data for Ac or Cb. Since the S-F peak for Ac (2.5 micron radius) is identical to four of the other cloud types it appears this value may have been obtained by association and it is probably incorrect also.

It should be noted that the Diem drop size data as reproduced in Mason (1957, 1971) incorrectly give radius as the drop-size parameter. Reference to Diem's original 1948 paper shows the size parameter is diameter, as reproduced by Fletcher (1962). This situation only affected the S-F mode radius for Cb (Cg) as can be seen in Table 12, where the S-F mode is twice the value from the Mason table.

Our recommendation then was to revise the S-F drop-size parameterizations to be based primarily on Diem's drop-size distributions, whose peak locations are consistent with recent measurements. Diem's Cg data were used for Cb, and As values were used for Ac. Our revised parameterizations for the S-F model used diameter as the size parameter.

A further test of the validity of the drop size distributions is whether the observed total droplet concentration is reproduced for an observed total LWC. We conducted this test on the revised S-F parameterizations and the results are presented below.

Observed droplet concentrations and the corresponding concentrations computed from the revised S-F parameterization are shown in Table 14. Each set of entries contains the computed concentration (obtained using the observed liquid water content as input) and the observed concentration and its liquid water content. The Diem concentrations were obtained from Mason (1971, p. 112). The correspondence between the data in the first two columns shows that the Calspan derived parameterizations reproduce fairly well Diem's observed total concentrations. One must recognize that Diem's data are averages and that any individual cloud probably will depart from these averages. In addition, Diem's data are for continental European clouds, whose nucleii populations may differ from those in other parts of the world.

Table 14 Total Droplet Concentration (Number/cm^3) for the LWC (g/m^3) in parentheses. Calculated values from the revised S-F parameterizations. Observations as indicated by reference number.

	Diem (1948)		More Recent	
Cloud Type	S-F Calculated	Observed	S-F Calculated	Observed
St	185 (.29)	260 (.29)	63 (.1)	200 (.1) Ref. (62)
As	355 (.28)	450 (.28)	-	-
Ns	212 (.40)	330 (.40)	-	-
Cu	1596 (.32)	1000 (.32)	798 (.16)	600 (.16) Ref. (29A)
Sc	317 (.09)	350 (.09)	2147 (.61)	200-300 (.61) Ref. (53)
Cb	490 (.87)	545 (.87)	-	-

For example, with reference to mode radii data presented in Table 12, consider the data values for the recent observations. For the stratus cloud, the computed concentration is about one-third of the average observed value. These observed values are for thin (200m) low-level stratus off the west coast of the US, with evidence that the drop size distributions are peaked at about half the revised S-F mode; thus, many

of these smaller droplets are needed to produce the observed liquid water relative to the number needed at the larger-size peak in the S-F parameterizations. The opposite effect can be seen in the Sc where the observed drop-size peak is larger than the S-F parameterization, and thus fewer drops are required to produce the observed liquid water.

In summary, we have generated a revised set of drop-size parameterizations, presented in Table 15, which are consistent in mode drop-size values and not inconsistent with observations of total concentration. For the intended application of the S-F model, to estimate conditions on a world-wide basis (i.e., ignoring nuclei population variations) from a single set of parameterizations, the parameterized values we have computed will serve well.

TABLE 15

Revised Parameters for Smith-Feddes
Cloud Drop Distribution Curves

CLOUD TYPE	a	P	V	X	B	S	M
ST	4.25	.0138	321.6	0-40	0	.1975	6
SC	3.25	.0748	143.8	0-25	0	.436	6
CU	3.75	.1150	220.9	0-20	0	.322	6
NS	3.5	.0064	179.6	0-40	0	.1575	6
AS	4.75	.0889	448.9	0-40	0	.124	36
AC	4.75	.0889	448.9	0-40	0	.124	36
CB	6.75	.0504	1288.2	0-40	0	.0593	36

a = Mode of drop-size distribution (radius(microns))

P = Percentage of condensed moisture content in one micron radius interval centered at mode (a)

V = Volume of droplet at mode, (micron^3)

X = Drop-size Range (radius(microns))

B = Location of origin of curve

S = Shape factor of the curve

M = Amplitude factor of the curve

3.6.2 Precipitation Drop Distribution

The equation for precipitation drop size which we derived from the Kessler (1969) equations matches the equation contained int he current Smith-Feddes computer code.

3.7 THERMODYNAMIC PHASE

In the S-F model, thermodynamic phase was defined as the percentage of total condensed moisture which was liquid water as opposed to ice. The percentages appear to be derived from curves (Khrgian, 1963) reproduced in Figure 5 in Smith (1974) which show percentage versus temperature in the range 0° to -40°C (Fig. 10). However, Curve 2, e.g., does not define the percentage of liquid water present in a cloud at a given temperature, but rather the percentage of occurrence of supercooled liquid clouds in all the clouds which were sampled, including those composed of mixed water and ice and all ice. Thus the estimates of the relative amounts of water and ice provided by the S-F model are based on inappropriate data and are thus unfounded.

The data set necessary to provide the relative percentages of water and ice in supercooled cloud has not been acquired. The measurements are difficult to obtain, requiring separate mass measurements of ice and water content, or either component and the total. Typically, ice crystal measurements are reported as number per cubic centimeter, with little or no information about the mass of ice crystals; and data for providing the relative percentages of ice and water in a cloud whose temperature is between 0°C and -40°C do not exist. However, available data do provide the probability that, at a given temperature, a cloud is all supercooled water, and the S-F output now provides this information as a probability of encounter.

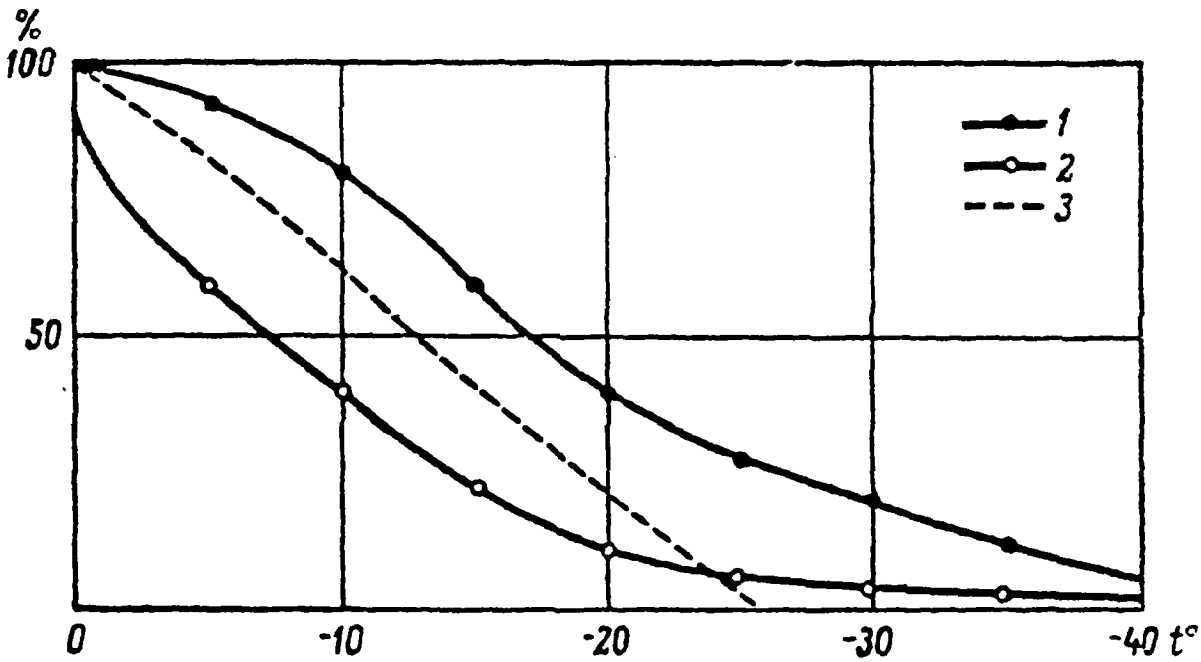

FIGURE 10. Average frequencies of appearance of the supercooled and mixed phases over Russia (after Khrgian, 1963).

1 – liquid and mixed clouds together; 2 – liquid clouds (after A.M. Borovikov and L.G. Sakhno); 3 – liquid clouds (after Peppler)

REFERENCES

Bolton, D., 1980: "The Computation of Equivalent Potential Temperature," Mon. Wea. Rev., July 1980, 108, pp. 1046-1053.

Brown, E., 1983: Observations Concerning CLOUDC (Smith-Feddes) Model, Letter of Transmittal, Contract No. N60921-81-C-A235 (A007) 23 June 1983. EG&G Washington Analytical Services Center, Inc., P.O. Box 552, Dahlgren, VA 22448.

Diem, M., 1948: "Messungen Der Grosse Von Wolkenelementen II," Meteorol. Rundsch., Vol. 1, pp. 261-273.

Dykton, M., S. Grimes and B. Hampton, 1984: Program CLOUDC Source Code, February 1984. EG&G Washington Analytical Services Center, Inc., P.O. Box 552, Dahlgren, VA, 22448.

Feddes, R.G., 1973: "A Technique to Specify Liquid Water Content at a Point in the Atmosphere," USAFETAC Project 6988, USAFETAC, Washington, D.C. 20333, 1973, (unpublished).

Feddes, R.G., 1974: "A Synoptic-Scale Model for Simulating Condensed Atmospheric Moisture," USAFETAC, Washington, D.C. 20333, June 1974.

Fletcher, N.H., 1962: The Physics of Rainclouds. Cambridge University Press, American Branch, 32 East 57th Street, New York, NY.

Haurwitz, B., 1941: Dynamic Meteorology. McGraw-Hill Book Company, Inc., New York, NY.

Jeck, R.K., 1983: "A New Data Base of Supercooled Cloud Variables for Altitudes up to 10,000 Ft AGL and the Implications for Low Altitude Aircraft Icing," Naval Research Laboratory, Washington, DC, Final Report, August 1983.

Kessler, E., 1969: "On the Continuity of Water Substance in Atmospheric Circulation," Meteorological Monographs, 10, No. 32, 1969, pp. 94. American Meteorological Society, 45 Beacon St., Boston, MA 02108.

Khrgian, A.K., 1963: "Cloud Physics," Israel Program for Scientific Translations, Jerusalem, 1963.

Mason, B.J., 1971: "The Physics of Clouds," Clarendon Press, Oxford, 2d Ed., 1971.

Smith, R.D., 1974: "Atmospheric Moisture Parameterization," USAF Environmental Technical Applications Center, Washington, DC, January 1974.

Warner, J., 1979: "On Steady-State One Dimensional Models of Cumulus Convection," J. Atmos. Sci., 1979, 27, pp. 1035-1040.

BIBLIOGRAPHY

RECENT LITERATURE

1. Baker, M.B., A.M. Blyth, D.J. Carruthers, S.J. Caughey, T.W. Choularton, B.J. Conway, G. Fullarton, M.J. Gay, J. Latham, C.S. Mill, M.H. Smith and I.M. Stromberg, "Field Studies of the Effect of Entrainment Upon the Structure of Clouds at Great Dunn Fell," Quart. J.R. Met. Soc., 1982, 108, pp. 899-916.

2. Bennetts, D.A. and M. Ouldridge, "An Observational Study of the Anvil of a Winter Maritime Cumulonimbus Cloud," Quart. J.R. Met. Soc., 1984, 110 , pp. 85-103.

3. Bennetts, D.A. and P. Ryder, "A Study of Mesoscale Convective Bands Behind Cold Fronts. Part II: Cloud and Microphysical Structure," Quart. J.R. Met. Soc., 1984, 110, pp. 467-487.

4. Blyth, A.M., T.W. Choularton, G. Fullarton, J. Latham, C.S. Mill, M.H. Smith and I.M. Stromberg, "The Influence of Entrainment on the Evolution of Cloud Droplet Spectra: II. Field Experiments at Great Dunn Fell," Quart. J.R. Met. Soc., 1980, 106, pp. 821-840.

5. Boatman, J.F. and A.H. Auer, Jr., "The Role of Cloud Top Entrainment in Cumulus Clouds," J. Atmos. Sci., 1983, 40, pp. 1517-1534.

6. Breed, D.W., "Liquid Water Measurements in High Elevation Continental Cumuli," National Center for Atmospheric Research, Boulder, CO, Dec. 79.

7. Caughey, S.J. and M. Kitchen, "Simultaneous Measurements of the Turbulent and Microphysical Structure of Nocturnal Stratocumulus Cloud," Quart. J.R. Met. Soc., 1984, 110, pp. 13-34.

8. Cooper, W.A. and C.P.R. Saunders, "Winter Storms Over the San Juan Mountains. Part II: Microphysical Processes," J. Appl. Meteor.,1980, 19, pp. 927-941

9. Cooper, W.A. and G. Vali, "The Origin of Ice in Mountain Cap Clouds," J. Atmos. Sci., 1981, 38, pp. 1244-1259.

10. Corkum, D.A. and R.L. Lavoie, "Studies of the Microphysics of Clouds. Part II: Application of a Simple Cumulus Model to Trade Wind Cumulus," Dept. of Meteorology, Pennsylvania State University, Report No. 16, Final Report NSF GA-3956, pp. 175.

11. Daum, P.H., S.E. Schwartz and L. Newman, "Studies of the Gas- and Aqueous-Phase Composition of Stratiform Clouds," Presented at the 4th International Conference on Precipitation Scavenging, Dry Deposition and Resuspension, Santa Monica, California, 29 November-3 December 1982. Elsevier Science Publishing Co. Inc., 52 Vanderbilt Ave., New York, N.Y. 10017.

12. Desert Research Institute, "Project Skywater," Laboratory of Atmospheric Physics, University of Nevada System, P.O. Box 60220, Reno, NV 89506, June 1972.

13. Dye, J.E., "The Microphysical Structure of the 7 August 1979 New Mexico Thunderstorm," Proceedings in Atmospheric Electricity, 1983, pp. 304-307. A. Deepak Publishing, P.O. Box 7390, Hampton, VA 23666,

14. Dye, J.E., B.E. Martner and L.J. Miller, "Dynamical-Microphysical Evolution of a Convective Storm in a Weakly-Sheared Environment. Part I: Microphysical Observations and Interpretation," J. Atmos. Sci., 1983, 40, pp. 2083-2096.

15. Dye, J.E., L.J. Miller, B.E. Martner and Z. Levin, "Case Studies on Convective Storms. Case Study 6: 25 July 1976. Dynamical-Microphysical Evolution of a Convective Storm," NCAR, ATM-77-23757, May 1980.

16. Dyer, R.M. and I.D. Cohen, "Changes in the Nature of Fluctuations of Temperature and Liquid Water Content During the Life time of a Large-Scale Winter Storm," J. Climate Appl. Meteor., 1983, 22, pp. 385-393.

17. Feigelson, E.M., 'Preliminary Radiation Model of a Cloudy Atmosphere. Part I-Structure of Clouds and Solar Radiation," Institute of Atmospheric Physics Academy of Sciences of the USSR, Moscow, 1977.

18. Gayet, J.F. et R.G. Soulage, "Heterogeneite Spatiale Des Proprietes Microphyosiques D un Cumulus Congestus," J. Rech. Atmos., X (1976), n°3, pp. 157-173.

19. Heaps, M.G., "A Vertical Structure Algorithm for Low Visibility/Low Stratus Conditions," U.S. Army Atmospheric Sciences Laboratory, White Sands Missile Range, NM, June 1982.

20. Heggli, M.F. and L. Vardiman, "Supercooled Liquid Water and Ice Crystal Distributions within Sierra Nevada Winter Storms," J. Climate Appl. Meteor., 1983, 22, pp. 1875-1886.

21. Herman, G.F. and J.A. Curry, "Observational and Theoretical Studies of Solar Radiation in Arctic Stratus Clouds," J. Climate Appl. Meteor., 1984, 23, pp. 5-24.

22. Heymsfield, A.J., "Cirrus Uncinus Generating Cells and the Evolution of Cirriform Clouds. Part I: Aircraft Observations Growth of the Ice Phase," J. Atmos. Sci., 1975, 32, pp. 799-808.

23. Heymsfield, A.J., "Precipitation Development in Stratiform Ice Clouds: A Microphysical and Dynamical Study," J. Atmos. Sci., 1977, 34, pp. 367-381.

24. Heymsfield. A.J. and S. Howard, "Water Content Values Predicted from Radiosonde Data at Wallops Island for Selected Cases 1971-1974," Meteorology Research Inc., MRI 75 R-1311, March 1975.

25. Heymsfield, A.J., P.N. Johnson and J.E. Dye, "Observations of Moist Adiabatic Ascent in Northeast Colorado Cumulus Congestus Clouds," J. Atmos. Sci., 1978, 35, pp. 1689-1703.

26. Heymsfield, A.J. and R.G. Knollenberg, "Properties of Cirrus Generating Cells," J. Atmos. Sci., 1972, 29, pp. 1358-1366.

27. Hobbs, P.V., L.F. Radke, and D.G. Atkinson, "Airborne Measurements and Observations in Cirrus Clouds," Cloud Physics Group, University of Washington, 13 January 1975.

28. Hobbs, P.V., R.A. Houze, Jr., J.D. Locatelli, P.H. Herzegh, D.G. Atkinson, L.F. Radke, R.R. Weiss and K. Biswas, "Dynamical and Microphysical Structures of Cyclonic Storms in the Pacific Northwest (The Cycles Project)," Cloud Physics Group, University of Washington, Seattle, WA 98195, 23 April 1976.

29. Hobbs, P.V., L.F. Radke, A.B. Fraser, J.D. Locatelli, C.E. Robertson, D.G. Atkinson, R.J. Farber, R.R. Weiss, and R.C. Easter, "Studies of Winter Cyclonic Storms over the Cascade Mountain (1970-1971)." Contributions from the Cloud Physics Group, Research Report VI, University of Washington, Seattle, WA 98195, December 1971.

29A. Hosler, C.L., L.G. Davis, J.I. Kelley and E.J. Mack, 1967: "An Investigation of the Dynamics and Microphysics of Clouds." NSF Report #10 and Final Report NSF GP-4743. Penn St., University Park, PA 16802.

30. Houze, R.A., Jr., S.A. Rutledge, T.J. Matejka and P.V. Hobbs, "The Mesoscale and Microscale Structure and Organization of Clouds and Precipitation in Midlatitude Cyclones. III: Air Motions and Precipitation Growth in a Warm-Frontal Rainband," J. Atmos. Sci., 1981, 38, pp. 639-649.

31. Isaac G.A. and R.S. Schemenauer, "Large Particles in Supercooled Regions of Northern Canadian Cumulus Clouds," J. Appl. Meteor., 1979, 18, pp. 1056-1065.

32. Jeck, R.K., "A New Data Base of Supercooled Cloud Variables for Altitudes up to 10,000 Ft AGL and the Implications for Low Altitude Aircraft Icing," Naval Research Laboratory, Washington, DC, Final Report, August 1983.

33. Jordan, J., J. Hallett, and R. Reinking, "FACE-2 Data Reductions and Analyses (Prior to Disclosure of the Treatment Decision). Part IV: FACE-2 Microphysical Data for Analyses of Seeded and Unseeded Cumulus Towers," NOAA, Environmental Research Laboratories, October 1981.

34. Keller, V.W. and R.I. Sax, "Microphysical Development of a Pulsating Cumulus Tower: A Case Study," Quart. J.R. Met. Soc., 1981, 107, pp. 679-697.

34A. Kitchen, M. and S.J. Caughey, "Tethered-Balloon Observations of the Structure of Small Cumulus Clouds," Quart. J.R. Met. Soc., 1981, 107, pp. 853-874.

35. Lamb, D., K.W. Nielsen, H.E. Klieforth and J. Hallett, "Measurements of Liquid Water Content in Winter Cloud Systems Over the Sierra Nevada," J. Appl. Meteor., 1976, 15, pp. 763-775.

36. Long, A.B., "Preliminary Cloud Microphysics Studies for Texas HIPLEX 1979," Dept. of Meteorology, Texas A&M University, College Station, TX. March 1980.

37. Mossop, S.C., "Microphysical Properties of Supercooled Cumulus Clouds in which an Ice Particle Multiplication Process Operated," Quart. J.R. Met. Soc., 1985, 111, pp. 183-198.

38. Murty, A.S. Ramachandra, A.M. Selvam, R. Vijayakumar, S.K. Paul and Bh. V. Ramana Murty, "Electrical and Microphysical Measurements in Warm Cumulus Clouds Before and After Seeding," J. Appl. Meteor., 1976, 15, pp. 1296-1301.

39. Nicholls, S., "The Dynamics of Stratocumulus: Aircraft Observations and Comparisons with a Mixed Layer Model," Quart. J.R. Met. Soc., 1984, 110, pp. 783-820.

40. Noonkester, V. Ray, "Acrosol Size Spectra in a Convective Marine Layer with Stratus: Results of Airborne Measurements near San Nicolas Island, California," J. Appl. Meteor., 1981, 20, pp. 1076-1080.

41. Pace, John C., "Microphysical and Thermodynamic Characteristics Through the Melting Layer," Dept. of Atmospheric Science, University of Wyoming, November 1980.

42. Parltridge, G.W., "Infrared Emissivity, Short-Wave Albedo, and the Microphysics of Stratiform Water Clouds," J. Geophys. Res., 1974, 79, pp. 4053-4058.

43. Paltridge, G.W. and C.M.R. Platt, "Aircraft Measurements of Solar and Infrared Radiation and the Microphysics of Cirrus Cloud," Quart. J.R. Met. Soc., 1981, 107, pp. 367-380.

44. Parungo, F., C. Nagamoto, R. Schnell, I. Nolt, E. Nickerson, and W. Caldwell, "Hawaii Mesoscale Energy and Climate Project (HAMEC). III. Atmospheric Aerosol and Cloud Microphysics Measurements," NOAA, Environmental Research Laboratories, Boulder, CO 80303. March 1981.

45. Personne, P. et J.-L. Brenguier, "Heterogeneite De La Distribution Spatiale De La Teneur En Eau Dans Des Stratocumu,lus Et Cumulus. Observation De Spectres Bimodauxo Leur Relation Avec L Entrainement," J. Rech. Atmos., 17 (1983), n°3, pp. 223-238.

46. Plank, V.G., "Liquid-Water-Content and Hydrometeor Size-Distribution Information for the SAMS Missile Flights of the 1971-72 Season at Wallops Island, Virginia - AFCRL/SAMS Report Number 3," Air Force Cambridge Research Laboratories, L.G. Hanscom Field, MA 01731, July 1974.

47. Plank, V.G., "Hydrometeor Data and Analytical-Theoretical Investigations Pertaining to the SAMS Rain Erosion Program of the 1972-73 Season at Wallops Island, Virginia - AFGL/SAMS Report No. 5," Air Force Geophysics Laboratory, Hanscom AFB, MA 01731, July 1977.

48. Platt, C.M.R., "Infrared Absorption" and Liquid Water Content in Stratocumulus Clouds," Quart. J.R. Met. Soc., 1976, 102, pp. 553-561.

49. Rangno, A.L., P.V. Hobbs, and L.F. Radke, "Tracer and Diffusion and Cloud Microphysical Studies in the American River Basin," Cloud Physics Group, University of Washington, Seattle, WA 98195, August 1977.

50. Sartor, J.D. and T.W. Cannon, "Collating Airborne and Surface Observations of the Microstructure of Precipitating Continental Convective Clouds," J. Appl. Meteor., 1977, 16, pp. 697-707.

51. Sax, R.I., J. Thomas, M. Bonebrake, and J. Hallett, "Ice Evolution within Seeded and Nonseeded Florida Cumuli," J. Appl. Meteor., 1979, 18, pp. 203-214.

52. Schmetz, J., E. Raschke and H. Fimpel, "Solar and Thermal Radiation in Maritime Stratocumulus Clouds," Beitr. Phys. Atmosph., Vol. 54, November 1981, pp. 442-452.

53. Slingo, A., R. Brown and C.L. Wrench, "A Field Study of Nocturnal Stratocumulus; III. High Resolution Radiative and Microphysical Observations," Quart. J.R. Met. Soc, 1982, 108, pp. 145-165.

54. Slingo, A., S. Nicholls, and J. Schmetz, "Aircraft Observations of Marine Stratocumulus During JASIN," Quart. J.R. Met. Soc, 1982, 108, pp. 833-856.

55. Snider, J.B. and D.C. Hogg, "Ground-Based Radiometric Observations of Cloud Liquid in the Sierra Nevada," NOAA, Environmental Research Laboratories, Boulder, CO 80303, May 1981.

56. Soulage, R.G., P. Personne et J.L. Brenguier, "Particules Precipitantes Dans Des Stratocumulus Peu Epais Au-Dessus De Valladolid: Concequences Pouro La Modifiabilite Des Nuages Dans Pap," J. Rech. Atmos., 15 (1981), n°2, pp. 131-142.

57. Spyers-Duran, P., "Systematic Measurements of Cloud Particle Spectra in Middle Level Clouds," Dept. of the Geophysical Sciences, University of Chicago, IL 60637, May 1972.

58. Stephens, G.L., G.W. Paltridge and C.M.R. Platt, "Radiation Profiles in Extended Water Clouds. III: Observations," J. Atmos. Sci., 1978, 35, pp. 2133-2141.

59. Stewart, R.E. and J.D. Marwitz, "Microphysical Effects of Seeding Wintertime Stratiform Clouds Near the Sierra Nevada Mountains," J. Appl. Meteor., 1982, 21, pp. 874-880.

60. Takeuchi, D.M., "Microphysics Observations of Convective Clouds in the Texas HIPLEX Area," Meteorology Research, Inc., Box 637, Altadena, CA 91001, July 1980.

61. Telford, J.W. and P.B. Wagner, "The Dynamical and Liquid Water Structure of the Small Cumulus as Determined from its Environment," Pure and Applied Geophysics, 1980, Vol 118, pp. 935-952.

62. Telford, J.W. and P.B. Wagner, "Observations of Condensation Growth Determined by Entity Type Mixing," Pure and Applied Geophysics, 1981, Vol. 119, pp. 934-965.

63. Twomey, S., "Radiative Effects in California Stratus," Beitr. Phys. Atmosph. Vol. 56, No. 4, November 1983, pp. 429-439.

64. Varley, D.J., "Cirrus Particle Distribution Study, Part 1," Air Force Geophysics Laboratory, Hanscom AFB, MA 01731, August 1978.

65. Varley, D.J., "Microphysical Properties of a Large Scale Cloud System, 1-3 March 1978," Air Force Geophysics Laboratory, Hanscom AFB, MA 01731, January 1980.

66. Varley, D.J. and D.M. Brooks, "Cirrus Particle Distribution Study, Part 2," Air Force Geophysics Laboratory, Hanscom AFB, MA 01731, October 1978.

67. Wang, P. and P.V. Hobbs, "The Mesoscale and Microscale Structure and Organization of Clouds and Precipitation in Midlatitude Cyclones. X: Wavelike Rainbands in an Occlusion," J. Atmos. Sci., 1983, 40, pp. 1950-1963.

68. Warner, J., "On Steady-State One-Dimensional Models of Cumulus Convection," J. Atmos. Sci., 1970, 27, pp. 1035-1040.

69. Warner, J.,"Time Variation of Updraft and Water Content in Small Cumulus Clouds," J. Atmos. Sci., 1977, 34, pp. 1306-1312.

70. Wilson, G.W. and Ralph Woratschek, "Microphysical Properites of Artificial and Natural Clouds and Their Effects on UH-1H Helicopter Icing," US Army

Aviation Engineering Flight Activity, Edwards Air Force Base, CA 93523, Final Report, August 1979.

ORIGINAL LITERATURE REVIEWED WHICH WAS USED IN THE DEVELOPMENT AND REPORTING OF THE SMITH FEDDES MODEL

71. Ackerman, B., "Some Observations of Water Contents in Hurricanes," J. Atmos. Sci., 1963, 20, pp. 288-298.

72. Blau, H.H., Jr., et al., "Cloud Microstructure Studies," Contract No. NAS 5-21696, NASA, Greenbelt MD, November 1972.

73. Byers, H.R., "Elements of Cloud Physics," The University of Chicago Press, Chicago, IL, 1965.

74. Chang, D.T., and J.H. Willand, "Further Developments in Cloud Statistics for Computer Simulation," Final Report Contract No. NAS 8-26847, NASA, Huntsville, AL 35812, March 1972.

75. Diem, M., "Messungen Der Grosse Von Wolkenelementen II," Meteorol. Rundsch., Vol. 1, 1948, pp. 261-273.

76. Feddes, R.G., "A Technique to Specify Liquid Water Content at a Point in the Atmosphere," USAFETAC Project 6988, USAFETAC, Washington, D.C. 20333, 1973, (unpublished).

77. Feddes, R.G., "A Synoptic-Scale Model for Simulating Condensed Atmospheric Moisture," USAFETAC, Washington, D.C. 20333, June 1974.

78. Kessler, E., "On the Continuity of Water Substance in Atmospheric Circulation," Meteorological Monographs, 10, No. 32, 1969, pp. 94. American Met. Soc., 45 Beacon St., Boston, MA 02108.

79. Khrgian, A.K., "Cloud Physics," Israel Program for Scientific Translations, Jerusalem, 1963.

80. Mason, B.J., "The Physics of Clouds," Clarendon Press, Oxford, 2d Ed., 1971.

81. Ryan R.T., H.H. Blau, Jr., P.C. von Thuna and M.L. Cohen, "Cloud Microstructure as Determined by an Optical Cloud Particle Spectrometer," J. Appl. Meteor., 1972, 11, pp. 149-156.

82. Smith, Robert D., "Atmospheric Moisture Parameterization," USAF Environmental Technical Applications Center, Washington, D.C. 20333, January 1974.

Appendix A

VERTICAL PROFILES OF CONDENSED MOISTURE CONTENT ORIGINALLY USED IN SMITH-FEDDES MODEL

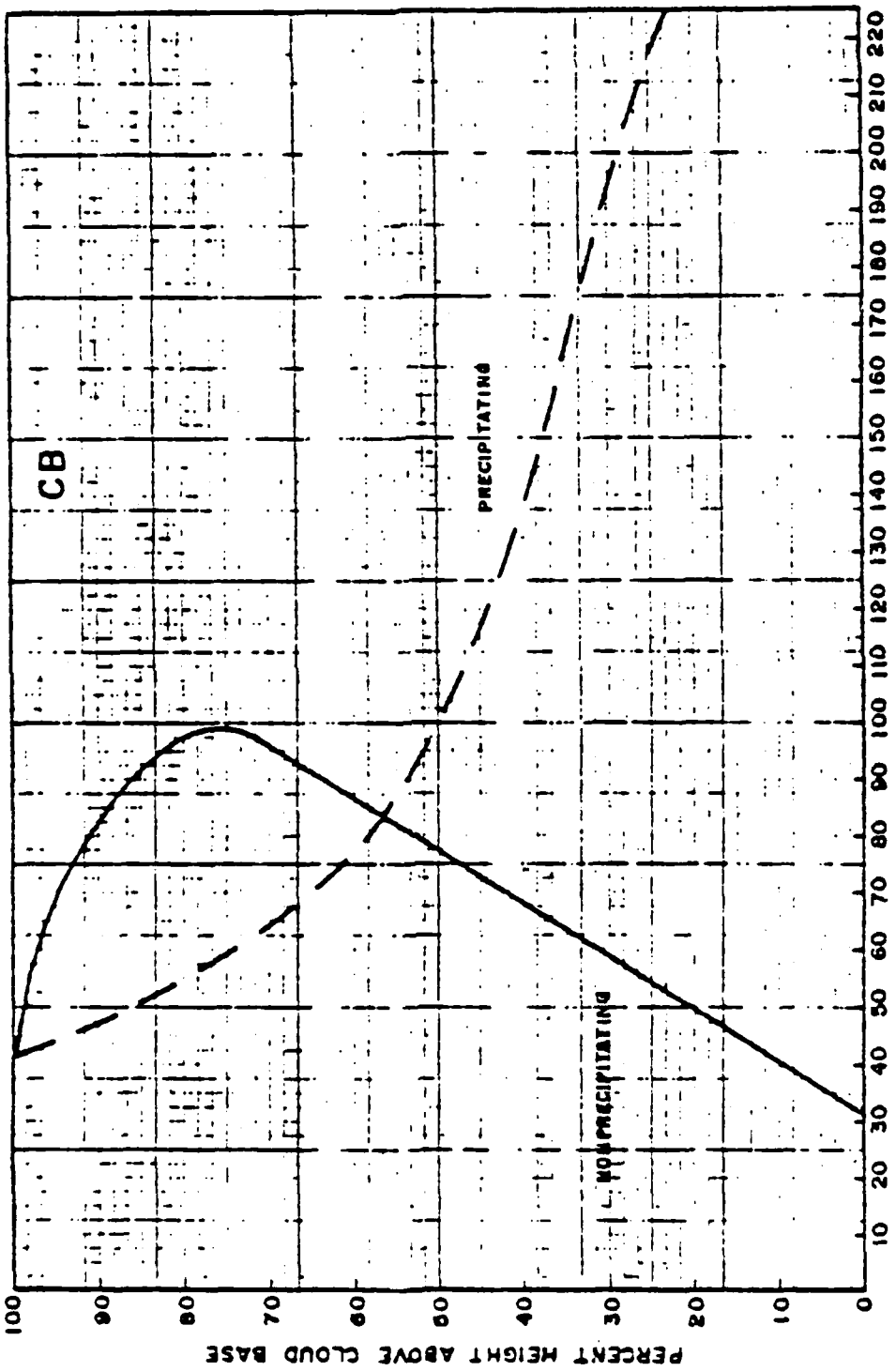

Figure A-1. Vertical Cloud Profile, Cumulonimbus (CB).

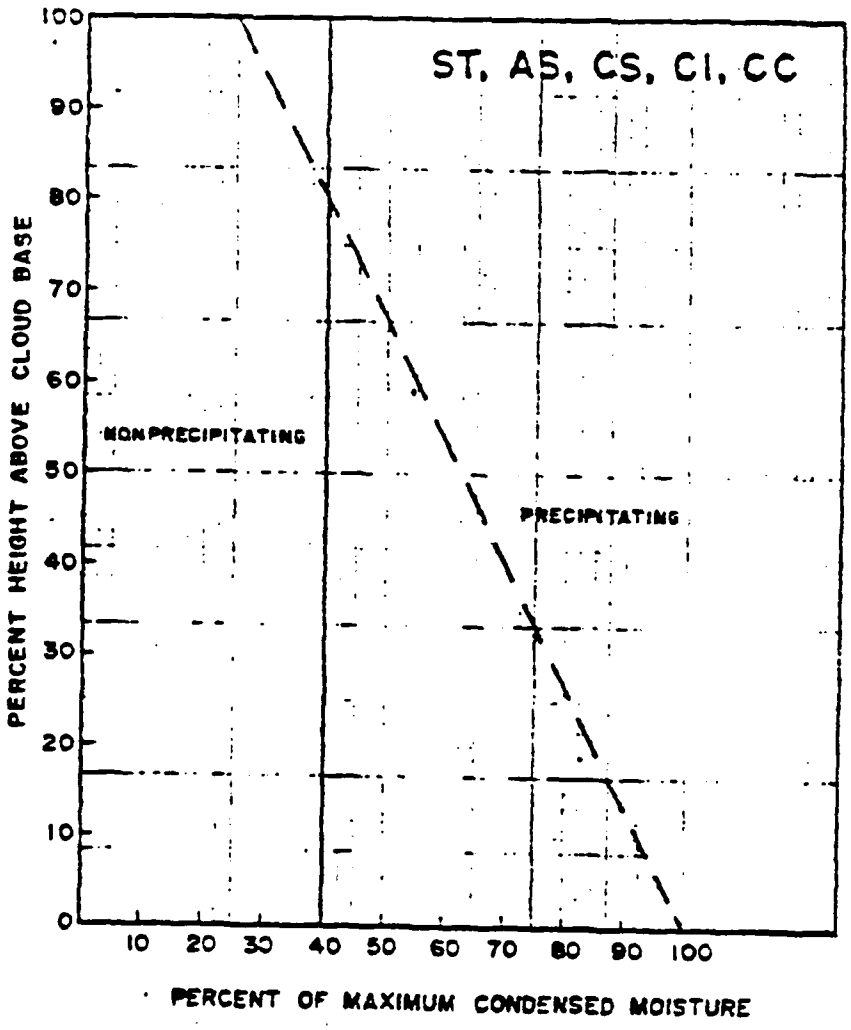

Figure A-2 . Vertical Cloud Profile, ST, AS, CS, CI, CC.

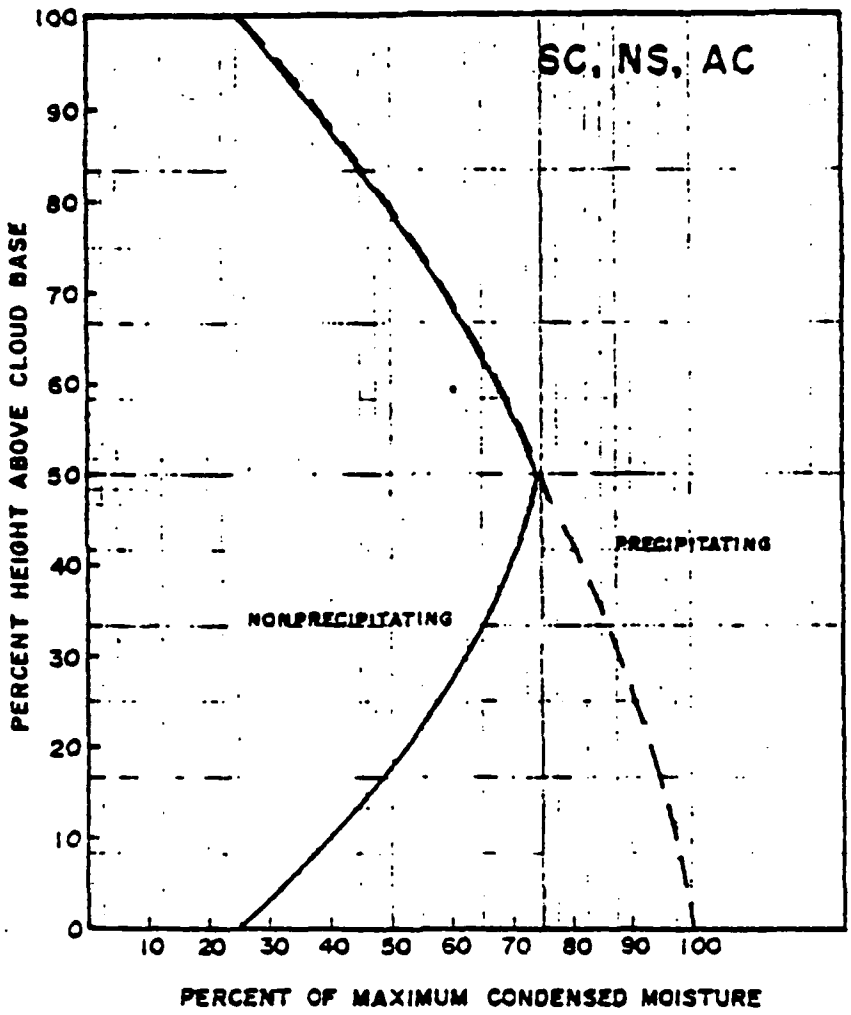

Figure A-3 . Vertical Cloud Profile, SC, NS, AC.

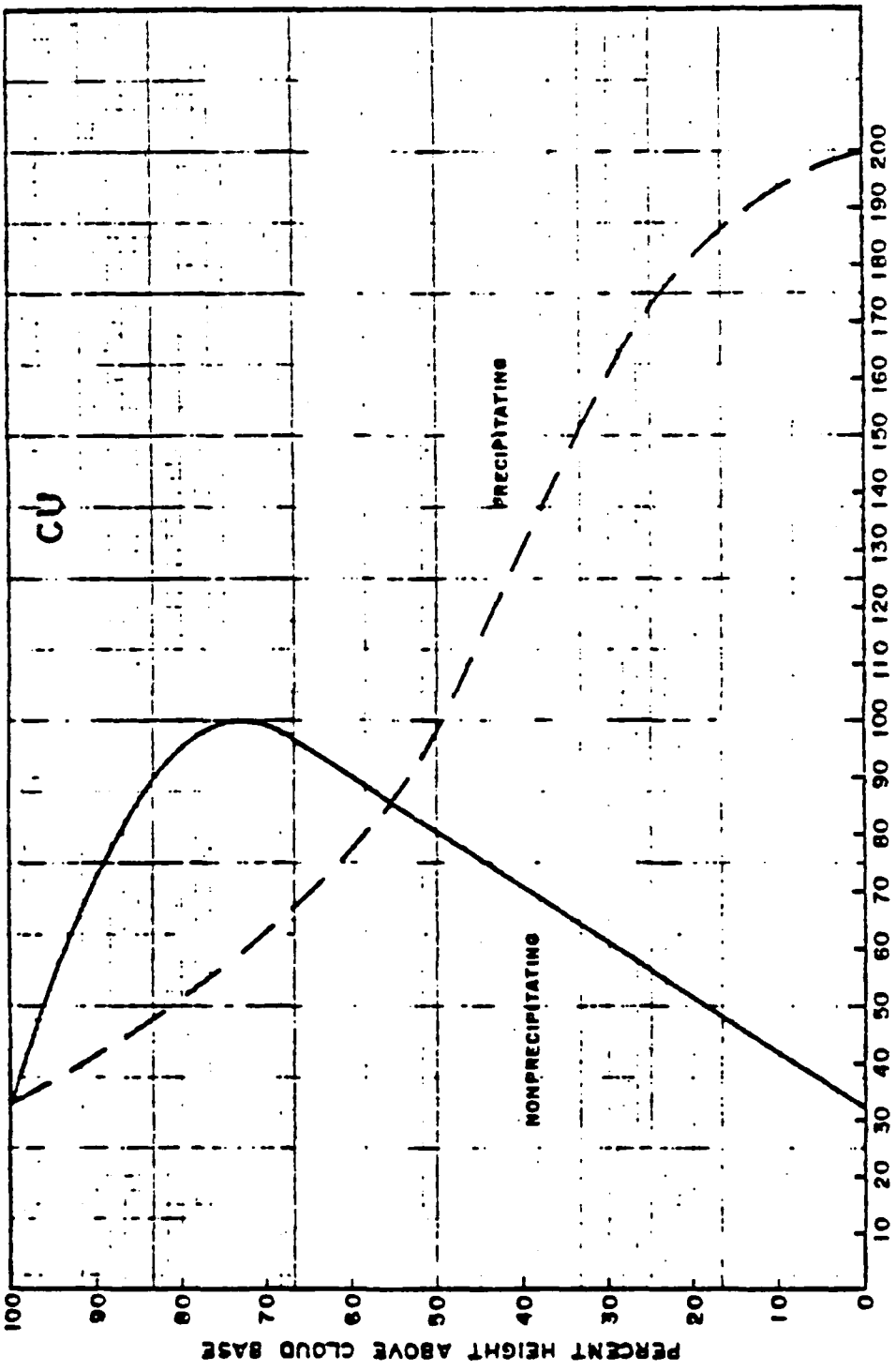

Figure A-4. Vertical Cloud Profile, Cumulus (CU).

APPENDIX B

TABULATION OF CONDENSED MOISTURE CONTENT AND CLOUD HEIGHT DATA FOUND DURING LITERATURE SEARCH

REF NO.	CLOUD TYPE	BASE HEIGHT (Km)	TOP HEIGHT (Km)	BASE TEMP ('C)	TOP TEMP ('C)
21	St	0.657	0.892		

HEIGHT (Km)	CMC (G/M3)	% HEIGHT ABOVE BASE	% CMC OF MAX
0.892	0.000	100.0	0.0
0.892	0.021	100.0	21.9
0.862	0.096	87.2	100.0
0.773	0.056	49.4	58.3
0.677	0.013	8.5	13.5
0.657	0.000	0.0	0.0

REF NO.	CLOUD TYPE	BASE HEIGHT (Km)	TOP HEIGHT (Km)	BASE TEMP ('C)	TOP TEMP ('C)
21	St	0.500	0.883		

HEIGHT (Km)	CMC (G/M3)	% HEIGHT ABOVE BASE	% CMC OF MAX
0.883	0.000	100.0	0.0
0.880	0.112	99.2	39.0
0.851	0.287	91.6	100.0
0.753	0.066	66.1	23.0
0.550	0.019	13.1	6.6
0.500	0.000	0.0	0.0

REF NO.	CLOUD TYPE	BASE HEIGHT (Km)	TOP HEIGHT (Km)	BASE TEMP ('C)	TOP TEMP ('C)
21	St	0.030	0.272		

HEIGHT (Km)	CMC (G/M3)	% HEIGHT ABOVE BASE	% CMC OF MAX
0.272	0.000	100.0	0.0
0.272	0.041	100.0	10.4
0.233	0.393	83.9	100.0
0.100	0.175	28.9	44.5
0.030	0.000	0.0	0.0

REF NO.	CLOUD TYPE	BASE HEIGHT (Km)	TOP HEIGHT (Km)	BASE TEMP (°C)	TOP TEMP (°C)
21	St	1.090	1.316		

HEIGHT (Km)	CMC (G/M3)	% HEIGHT ABOVE BASE	% CMC OF MAX
1.316	0.000	100.0	0.0
1.316	0.040	100.0	10.2
1.187	0.394	42.9	100.0
1.125	0.159	15.5	40.4
1.104	0.026	6.2	6.6
1.090	0.000	0.0	0.0

REF NO.	CLOUD TYPE	BASE HEIGHT (Km)	TOP HEIGHT (Km)	BASE TEMP (°C)	TOP TEMP (°C)
21	As	3.354	3.530		

HEIGHT (Km)	CMC (G/M3)	% HEIGHT ABOVE BASE	% CMC OF MAX
3.530	0.000	100.0	0.0
3.530	0.026	100.0	25.2
3.502	0.103	84.1	100.0
3.450	0.061	54.5	59.2
3.382	0.020	15.9	19.4
3.354	0.000	0.0	0.0

REF NO.	CLOUD TYPE	BASE HEIGHT (Km)	TOP HEIGHT (Km)	BASE TEMP (°C)	TOP TEMP (°C)
21	St	1.400	1.839		

HEIGHT (Km)	CMC (G/M3)	% HEIGHT ABOVE BASE	% CMC OF MAX
1.839	0.000	100.0	0.0
1.839	0.061	100.0	59.2
1.749	0.103	79.5	100.0
1.595	0.092	44.4	89.3
1.425	0.054	5.7	52.4
1.400	0.000	0.0	0.0

REF NO.	CLOUD TYPE	BASE HEIGHT (Km)	TOP HEIGHT (Km)	BASE TEMP ('C)	TOP TEMP ('C)
21	St	0.220	0.466		

HEIGHT (Km)	CMC (G/M3)	% HEIGHT ABOVE BASE	% CMC OF MAX
0.466	0.000	100.0	0.0
0.466	0.095	100.0	69.3
0.446	0.137	91.9	100.0
0.300	0.024	32.5	17.5
0.220	0.000	0.0	0.0

REF NO.	CLOUD TYPE	BASE HEIGHT (Km)	TOP HEIGHT (Km)	BASE TEMP ('C)	TOP TEMP ('C)
21	St	0.810	1.200		

HEIGHT (Km)	CMC (G/M3)	% HEIGHT ABOVE BASE	% CMC OF MAX
1.200	0.000	100.0	0.0
1.189	0.627	97.2	100.0
1.080	0.442	69.2	70.5
0.972	0.301	41.5	48.0
0.825	0.043	3.8	6.9
0.810	0.000	0.0	0.0

REF NO.	CLOUD TYPE	BASE HEIGHT (Km)	TOP HEIGHT (Km)	BASE TEMP ('C)	TOP TEMP ('C)
21	St	0.810	1.190		

HEIGHT (Km)	CMC (G/M3)	% HEIGHT ABOVE BASE	% CMC OF MAX
1.190	0.000	100.0	0.0
1.052	0.150	63.7	36.9
0.957	0.407	38.7	100.0
0.843	0.034	8.7	8.4
0.810	0.000	0.0	0.0

REF NO.	CLOUD TYPE	BASE HEIGHT (Km)	TOP HEIGHT (Km)	BASE TEMP (°C)	TOP TEMP (°C)
21	St	0.688	0.980		

HEIGHT (Km)	CMC (G/M3)	% HEIGHT ABOVE BASE	% CMC OF MAX
0.980	0.000	100.0	0.0
0.975	0.465	98.3	100.0
0.846	0.265	54.1	57.0
0.731	0.027	14.7	5.8
0.688	0.000	0.0	0.0

REF NO.	CLOUD TYPE	BASE HEIGHT (Km)	TOP HEIGHT (Km)	BASE TEMP (°C)	TOP TEMP (°C)
21	St	0.705	1.026		

HEIGHT (Km)	CMC (G/M3)	% HEIGHT ABOVE BASE	% CMC OF MAX
1.026	0.000	100.0	0.0
1.022	0.352	98.8	80.9
0.971	0.435	82.9	100.0
0.850	0.289	45.2	66.4
0.724	0.023	5.9	5.3
0.705	0.000	0.0	0.0

REF NO.	CLOUD TYPE	BASE HEIGHT (Km)	TOP HEIGHT (Km)	BASE TEMP (°C)	TOP TEMP (°C)
21	St	0.804	1.089		

HEIGHT (Km)	CMC (G/M3)	% HEIGHT ABOVE BASE	% CMC OF MAX
1.089	0.000	100.0	0.0
1.089	0.051	100.0	11.1
1.035	0.458	81.1	100.0
0.924	0.160	42.1	34.9
0.807	0.021	1.1	4.6
0.804	0.000	0.0	0.0

REF NO.	CLOUD TYPE	BASE HEIGHT (Km)	TOP HEIGHT (Km)	BASE TEMP (°C)	TOP TEMP (°C)
21	As	4.390	4.648		

HEIGHT (Km)	CMC (G/M3)	% HEIGHT ABOVE BASE	% CMC OF MAX
4.648	0.000	100.0	0.0
4.648	0.083	100.0	92.2
4.602	0.090	82.2	100.0
4.505	0.048	44.6	53.3
4.395	0.026	1.9	28.9
4.390	0.000	0.0	0.0

REF NO.	CLOUD TYPE	BASE HEIGHT (Km)	TOP HEIGHT (Km)	BASE TEMP (°C)	TOP TEMP (°C)
58	St	1.070	1.470	1.8	-1.4

HEIGHT (Km)	CMC (G/M3)	% HEIGHT ABOVE BASE	% CMC OF MAX
1.460	0.065	97.5	24.3
1.370	0.267	75.0	100.0
1.280	0.267	52.5	100.0
1.190	0.181	30.0	67.8
1.100	0.133	7.5	49.8

REF NO.	CLOUD TYPE	BASE HEIGHT (Km)	TOP HEIGHT (Km)	BASE TEMP (°C)	TOP TEMP (°C)
58	St	1.130	1.610	-0.4	-2.6

HEIGHT (Km)	CMC (G/M3)	% HEIGHT ABOVE BASE	% CMC OF MAX
1.460	0.544	68.8	100.0
1.400	0.266	56.3	48.9
1.310	0.171	37.5	31.4
1.220	0.183	18.8	33.6
1.130	0.055	0.0	10.1

REF NO.	CLOUD TYPE	BASE HEIGHT (Km)	TOP HEIGHT (Km)	BASE TEMP (°C)	TOP TEMP (°C)
58	St	0.980	1.530	1.3	-2.1

HEIGHT (Km)	CMC (G/M3)	% HEIGHT ABOVE BASE	% CMC OF MAX
1.460	0.617	97.3	100.0
1.400	0.200	76.4	32.4
1.310	0.035	60.0	5.7
1.220	0.074	43.6	12.0
1.130	0.139	27.3	22.5
1.040	0.096	10.9	15.6

REF NO.	CLOUD TYPE	BASE HEIGHT (Km)	TOP HEIGHT (Km)	BASE TEMP (°C)	TOP TEMP (°C)
58	St	1.510	1.930	5.0	4.0

HEIGHT (Km)	CMC (G/M3)	% HEIGHT ABOVE BASE	% CMC OF MAX
1.780	0.244	84.4	100.0
1.680	0.207	53.1	84.8
1.600	0.140	28.1	57.4
1.540	0.123	9.4	50.4
1.510	0.102	0.0	41.8

REF NO.	CLOUD TYPE	BASE HEIGHT (Km)	TOP HEIGHT (Km)	BASE TEMP (°C)	TOP TEMP (°C)
58	St	1.900	2.130	1.0	-1.0

HEIGHT (Km)	CMC (G/M3)	% HEIGHT ABOVE BASE	% CMC OF MAX
2.110	0.230	91.3	100.0
2.080	0.157	78.3	68.3
2.020	0.146	52.2	63.5
1.960	0.043	26.1	18.7

REF NO.	CLOUD TYPE	BASE HEIGHT (Km)	TOP HEIGHT (Km)	BASE TEMP (°C)	TOP TEMP (°C)
58	St	2.170	2.350	1.0	0.0

HEIGHT (Km)	CMC (G/M3)	% HEIGHT ABOVE BASE	% CMC OF MAX
2.320	0.242	83.3	100.0
2.260	0.212	50.0	87.6
2.190	0.025	11.1	10.3

REF NO.	CLOUD TYPE	BASE HEIGHT (Km)	TOP HEIGHT (km)	BASE TEMP (°C)	TOP TEMP (°C)
62	St	0.320	0.530	10.0	10.0

HEIGHT (Km)	CMC (G/M3)	% HEIGHT ABOVE BASE	% CMC OF MAX
0.530	0.000	100.0	0.0
0.525	0.310	97.6	100.0
0.320	0.000	0.0	0.0

REF NO.	CLOUD TYPE	BASE HEIGHT (Km)	TOP HEIGHT (Km)	BASE TEMP (°C)	TOP TEMP (°C)
52	Sc	0.550	0.910	6.5	3.7

HEIGHT (Km)	CMC (G/M3)	% HEIGHT ABOVE BASE	% CMC OF MAX
0.910	0.000	100.0	0.0
0.910	0.600	100.0	100.0
0.700	0.225	41.7	37.5
0.550	0.000	0.0	0.0

REF NO.	CLOUD TYPE	BASE HEIGHT (Km)	TOP HEIGHT (Km)	BASE TEMP (°C)	TOP TEMP (°C)
52	Sc	0.550	0.920		

HEIGHT (Km)	CMC (G/M3)	% HEIGHT ABOVE BASE	% CMC OF MAX
0.920	0.000	100.0	0.0
0.905	0.580	95.9	100.0
0.890	0.230	91.9	39.7
0.870	0.580	86.5	100.0
0.650	0.180	27.0	31.0
0.550	0.000	0.0	0.0

REF NO.	CLOUD TYPE	BASE HEIGHT (Km)	TOP HEIGHT (Km)	BASE TEMP (°C)	TOP TEMP (°C)
54	Sc	0.390	0.900	5.8	2.5

HEIGHT (Km)	CMC (G/M3)	% HEIGHT ABOVE BASE	% CMC OF MAX
0.900	0.000	100.0	0.0
0.845	0.580	89.2	90.6
0.810	0.640	82.4	100.0
0.490	0.100	19.6	15.6
0.390	0.000	0.0	0.0

REF NO.	CLOUD TYPE	BASE HEIGHT (Km)	TOP HEIGHT (Km)	BASE TEMP (°C)	TOP TEMP (°C)
48	Sc	2.000	2.415	7.5	7.5

HEIGHT (Km)	CMC (G/M3)	% HEIGHT ABOVE BASE	% CMC OF MAX
2.316	0.370	76.1	100.0
2.164	0.120	39.5	32.4
2.012	0.030	2.9	8.1

REF NO.	CLOUD TYPE	BASE HEIGHT (Km)	TOP HEIGHT (Km)	BASE TEMP (°C)	TOP TEMP (°C)
42	Sc	0.760	1.480	16.5	11.5

HEIGHT (Km)	CMC (G/M3)	% HEIGHT ABOVE BASE	% CMC OF MAX
1.480	0.000	100.0	0.0
1.330	0.250	79.2	100.0
0.760	0.000	0.0	0.0

REF NO.	CLOUD TYPE	BASE HEIGHT (Km)	TOP HEIGHT (Km)	BASE TEMP (°C)	TOP TEMP (°C)
53	Sc	0.607	0.963		

HEIGHT (Km)	CMC (G/M3)	% HEIGHT ABOVE BASE	% CMC OF MAX
0.963	0.000	100.0	0.0
0.963	0.430	100.0	100.0
0.810	0.210	57.0	48.8
0.783	0.120	49.4	27.9
0.711	0.100	29.2	23.3
0.607	0.000	0.0	0.0

REF NO.	CLOUD TYPE	BASE HEIGHT (Km)	TOP HEIGHT (Km)	BASE TEMP (°C)	TOP TEMP (°C)
53	Sc	0.801	0.998	4.0	2.7

HEIGHT (Km)	CMC (G/M3)	% HEIGHT ABOVE BASE	% CMC OF MAX
0.998	0.000	100.0	0.0
0.990	0.130	95.9	74.3
0.954	0.175	77.7	100.0
0.864	0.160	32.0	91.4
0.801	0.000	0.0	0.0

REF NO.	CLOUD TYPE	BASE HEIGHT (Km)	TOP HEIGHT (Km)	BASE TEMP ('C)	TOP TEMP ('C)
53	Sc	0.522	1.358	-1.3	-6.0

HEIGHT (Km)	CMC (G/M3)	% HEIGHT ABOVE BASE	% CMC OF MAX
1.358	0.000	100.0	0.0
1.340	0.080	97.8	5.3
1.330	1.520	96.7	100.0
1.200	0.500	81.1	32.9
1.130	0.930	72.7	61.2
0.909	0.390	46.3	25.7
0.837	0.600	37.7	39.5
0.801	0.390	33.4	25.7
0.522	0.000	0.0	0.0

REF NO.	CLOUD TYPE	BASE HEIGHT (Km)	TOP HEIGHT (Km)	BASE TEMP ('C)	TOP TEMP ('C)
39	Sc	0.400	0.800	10.7	8.8

HEIGHT (Km)	CMC (G/M3)	% HEIGHT ABOVE BASE	% CMC OF MAX
0.800	0.000	100.0	0.0
0.800	0.000	100.0	0.0
0.775	0.300	93.8	100.0
0.400	0.000	0.0	0.0
0.400	0.000	0.0	0.0

REF NO.	CLOUD TYPE	BASE HEIGHT (Km)	TOP HEIGHT (Km)	BASE TEMP ('C)	TOP TEMP ('C)
10	Cu	0.600	4.100		

HEIGHT (Km)	CMC (G/M3)	% HEIGHT ABOVE BASE	% CMC OF MAX
3.700	2.200	88.6	100.0
3.400	2.200	80.0	100.0
2.900	1.700	65.7	77.3
2.000	1.000	40.0	45.5
1.500	1.100	25.7	50.0
0.800	0.700	5.7	31.8

REF NO.	CLOUD TYPE	BASE HEIGHT (Km)	TOP HEIGHT (Km)	BASE TEMP ('C)	TOP TEMP ('C)
10	Cu	0.700	3.500		

HEIGHT (Km)	CMC (G/M3)	% HEIGHT ABOVE BASE	% CMC OF MAX
3.100	1.200	85.7	63.2
2.400	1.900	60.7	100.0
1.900	0.900	42.9	47.4
1.200	0.500	17.9	26.3
0.900	0.250	7.1	13.2

REF NO.	CLOUD TYPE	BASE HEIGHT (Km)	TOP HEIGHT (Km)	BASE TEMP ('C)	TOP TEMP ('C)
10	Cu	0.440	3.100		

HEIGHT (Km)	CMC (G/M3)	% HEIGHT ABOVE BASE	% CMC OF MAX
2.630	0.500	82.3	33.3
2.120	1.500	63.2	100.0
1.500	1.000	39.8	66.7
1.120	0.500	25.6	33.3
0.640	0.100	7.5	6.7

REF NO.	CLOUD TYPE	BASE HEIGHT (Km)	TOP HEIGHT (Km)	BASE TEMP ('C)	TOP TEMP ('C)
10	Cu	0.700	2.300		

HEIGHT (Km)	CMC (G/M3)	% HEIGHT ABOVE BASE	% CMC OF MAX
1.800	0.350	68.8	31.8
1.400	1.100	43.8	100.0
0.900	0.450	12.5	40.9

REF NO.	CLOUD TYPE	BASE HEIGHT (Km)	TOP HEIGHT (Km)	BASE TEMP (°C)	TOP TEMP (°C)
10	Cu	0.700	4.000		

HEIGHT (Km)	CMC (G/M3)	% HEIGHT ABOVE BASE	% CMC OF MAX
3.800	2.300	93.9	100.0
3.200	1.900	75.8	82.6
2.900	1.750	66.7	76.1
2.500	1.600	54.5	69.6
1.900	1.300	36.4	56.5
1.300	1.300	18.2	56.5
0.900	0.700	6.1	30.4

REF NO.	CLOUD TYPE	BASE HEIGHT (Km)	TOP HEIGHT (Km)	BASE TEMP (°C)	TOP TEMP (°C)
10	Cu	0.700	3.800		

HEIGHT (Km)	CMC (G/M3)	% HEIGHT ABOVE BASE	% CMC OF MAX
3.400	1.750	87.1	76.1
2.800	2.300	67.7	100.0
1.500	1.400	25.8	60.9
0.900	0.500	6.5	21.7

REF NO.	CLOUD TYPE	BASE HEIGHT (Km)	TOP HEIGHT (Km)	BASE TEMP (°C)	TOP TEMP (°C)
18	Cu	1.730	5.170	10.0	-10.0

HEIGHT (Km)	CMC (G/M3)	% HEIGHT ABOVE BASE	% CMC OF MAX
5.170	0.000	100.0	0.0
3.700	0.020	57.3	40.0
2.800	0.050	31.1	100.0
1.730	0.000	0.0	0.0

REF NO.	CLOUD TYPE	BASE HEIGHT (Km)	TOP HEIGHT (Km)	BASE TEMP (°C)	TOP TEMP (°C)
18	Cu	1.730	5.170	10.0	-10.0

HEIGHT (Km)	CMC (G/M3)	% HEIGHT ABOVE BASE	% CMC OF MAX
5.170	0.000	100.0	0.0
4.990	0.020	94.8	0.5
4.860	0.050	91.0	1.3
4.670	0.100	85.5	2.5
4.510	0.500	80.8	12.5
4.290	1.000	74.4	25.0
4.090	1.500	68.6	37.5
4.010	2.000	66.3	50.0
3.970	2.500	65.1	62.5
3.900	3.000	63.1	75.0
3.800	4.000	60.2	100.0
3.720	4.000	57.8	100.0
3.640	3.000	55.5	75.0
3.560	2.500	53.2	62.5
3.510	2.000	51.7	50.0
3.400	1.500	48.5	37.5
3.290	1.000	45.3	25.0
3.060	0.500	38.7	12.5
1.730	0.000	0.0	0.0

REF NO.	CLOUD TYPE	BASE HEIGHT (Km)	TOP HEIGHT (Km)	BASE TEMP (°C)	TOP TEMP (°C)
18	Cu	1.730	5.170	10.0	-10.0

HEIGHT (Km)	CMC (G/M3)	% HEIGHT ABOVE BASE	% CMC OF MAX
5.170	0.000	100.0	0.0
4.700	0.020	86.3	2.0
4.500	0.050	80.5	5.0
4.200	0.100	71.8	10.0
3.600	0.500	54.4	50.0
2.750	1.000	29.7	100.0
1.730	0.000	0.0	0.0

REF NO.	CLOUD TYPE	BASE HEIGHT (Km)	TOP HEIGHT (Km)	BASE TEMP (°C)	TOP TEMP (°C)
28	Cu	1.200	7.500		

HEIGHT (Km)	CMC (G/M3)	% HEIGHT ABOVE BASE	% CMC OF MAX
7.400	0.004	98.4	1.1
6.800	0.009	88.9	2.4
6.200	0.014	79.4	3.8
5.700	0.031	71.4	8.4
5.000	0.065	60.3	17.6
4.700	0.110	55.6	29.7
4.000	0.120	44.4	32.4
3.400	0.170	34.9	45.9
2.900	0.220	27.0	59.5
2.300	0.280	17.5	75.7
1.700	0.370	7.9	100.0